DYNAMICAL EFFECTS OF NOISE ON NONLINEAR SYSTEMS

A THESIS

SUBMITTED TO THE DEPARTMENT OF PHYSICS

AND THE GRADUATE SCHOOL OF ENGINEERING AND SCIENCE

OF BILKENT UNIVERSITY

IN PARTIAL FULFILLMENT OF THE REQUIREMENTS

FOR THE DEGREE OF

MASTER OF SCIENCE

By

ÖZER DUMAN

August, 2014

I certify that I have read this thesis and that in my opinion it is fully adequate, in scope and in quality, as a thesis for the degree of Master of Science.

Assist. Prof. Dr. Giovanni Volpe (Advisor)

I certify that I have read this thesis and that in my opinion it is fully adequate, in scope and in quality, as a thesis for the degree of Master of Science.

Assoc. Prof. Dr. Fatih Ömer İlday

I certify that I have read this thesis and that in my opinion it is fully adequate, in scope and in quality, as a thesis for the degree of Master of Science.

Assoc. Prof. Dr. Mehmet Burçin Ünlü

Approved for the Graduate School of Engineering and Science:

Prof. Dr. Levent Onural
Director of the Graduate School

ABSTRACT

DYNAMICAL EFFECTS OF NOISE ON NONLINEAR SYSTEMS

ÖZER DUMAN
M.S. in Physics
Supervisor: Assist. Prof. Dr. Giovanni Volpe
August, 2014

Randomness and nonlinear dynamics consitute the most essential part of many events in nature. Therefore, a better and comprehensive understanding of them is a crucial step in describing natural phenomena as well as the prospect of predicting their future outcome. Besides the interest from a fundamental point of view, it is also useful in a wide variety of applications requiring delicate and careful use of energy. Especially recent advances in micro- and nano-scale technology requires harnessing the underlying noise itself as it is relatively hard to exert forces without damaging the system at that scale. The main aim of this work is to study the effects of noise on nonlinear dynamics. We show that the interplay between noise, nonlinearity and nonequilibrium conditions leads to a finite drift with the potential to change the dynamics of the system completely in a predictable and tunable fashion. We report that the noise-induced drift disrupts the phase space of a 2-D nonlinear system by shifting the fixed point by a finite amount which may result in dramatic alterations over the temporal behavior of the system. We track such alterations to several multi-dimensional model systems from ecology, soft matter and statistical physics. In a 2-D ecological model describing two species competing for the same resource, it is found that the system switches between coexistence and extinction states depending on the shift due to the noise-induced drift whereas for an aggregate of Brownian particles, it is shown that noise-induced drift selectively shifts the probability distribution in certain geometries which can be used in the realization of a microparticle sorter in the mould of Feynman ratchets. In the case of the aggregate consisting of microswimmers, tunable anomalous diffusion depending on the confinement length is reported.

Keywords: Stochastic differential equations, stochastic differential delay equations, nonlinear dynamics, diffusion processes, Brownian motion, microswimmers.

ÖZET

GÜRÜLTÜNÜN DOĞRUSAL OLMAYAN SİSTEMLER ÜZERİNDEKİ ETKİLERİ

ÖZER DUMAN
Fizik, Yüksek Lisans
Tez Yöneticisi: Assist. Prof. Dr. Giovanni Volpe
Ağustos, 2014

Raslantısallık ve doğrusal olmayan dinamikler doğada gerçekleşmekte olan birçok olayın özünü teşkil etmektedir. Bu anlamda, doğa olaylarını tasvir etme ve olası sonuçlarını öngörme noktasında bu iki olguyu daha iyi ve kapsamlı bir biçimde anlamak önem arz etmekte. Bilimsel temele ilişkin ilginin yanı sıra, bu anlama çabası enerjinin hassas ve dikkatli kullanımını gerektiren çeşitli uygulamalar için kullanışlıdır. Özellikle yakın zamanda mikro- ve nano-teknoloji alanında yaşanan gelişmeler, bu boyutlarda sisteme zarar vermeden kuvvet uygulamak göreli olarak zor olduğundan, arka plandaki gürültüyü enerji kaynağı olarak kullanmayı gerekli kılmıştır. Bu çalışmanın esas amacı gürültünün doğrusal olmayan dinamikler üzerindeki etkisini araştırmak. Bu çalışmada gürültü, doğrusal olmama ve denge dışı olma durumlarının birbiriyle etkileşimi, sistemin dinamiklerini öngörülebilir ve ayarlanabilir bir şekilde bütünüyle değiştirebilecek sonlu bir sürüklenmeye yol açabileceğini gösteriyoruz. Gürültü kaynaklı sürüklenme 2 boyutlu doğrusal olmayan bir sistemin faz uzayını sabit noktayı sonlu bir miktar kaydırmak suretiyle değiştirdiğinden, sistemin zaman içerisindeki davranışında dramatik değişimlere sebebiyet verebilir. Bu değişimleri ekoloji, yumuşak madde ve istatistiksel fizikten uyarladığımız çeşitli çok boyutlu modellerde gösteriyoruz. Aynı kaynak için mücadele etmekte olan iki türü içeren 2 boyutlu ekolojik bir model dahilinde, sistemin gürültü kaynaklı sürüklenmeye bağlı olarak, türlerin bir arada yaşadığı ve yok olduğu durumlar arasında geçiş yaptığını; bir araya getirilmiş Brown parçacıkları içinse, gürültü kaynaklı sürüklenmenin olasılık dağılımını belirli geometrilerde kaydırdığını, bunun Feynman çarkları yapısında mikroparçacık ayrıştırıcı yapmada kullanılabileceğini gösteriyoruz. Bir araya getirilmiş mikroyüzücüler içinse, hapsedilme uzunluğuna bağlı anomal difüzyon gözlemlediğimizi rapor ediyoruz.

Anahtar sözcükler: Stokastik diferansiyel denklemler, gecikmeli stokastik diferansiyel denklemler, doğrusal olmayan dinamikler, difüzyon süreçleri, Brown hareketi, mikroyüzücüler.

Acknowledgement

I feel extremely privileged for having the chance to work with such a brilliant scientist and leader as Dr. Giovanni Volpe, whose extraordinary vision with a never-ending catalog of out-of-the-box ideas and infinite patience always motivated me to do better in science and in life. His generosity in sharing his experience, confidence, enthusiasm and ambition not only helped me grow as a researcher, but also inspired me as a person to attach meaning and pure joy with doing what you enjoy the most!

I am very much indebted to Dr. Ömer Ilday who has been the biggest influence in my life with his vision and the way he carries it out. It has been both exciting and rewarding for me to learn from a person who is like those 19th-century-geniuses we can only read in books, with his vast knowledge, extraordinary imagination and the talent he shows in blending the two to do the courageous job of revolutionary science!

I would like to thank all of the group members in Soft Matter Lab and my department colleagues for creating such a good atmosphere to do research. It is necessary for me to single out Dr. Agnese Callegari's contributions which helped all of us a lot with EVERYTHING!

I am very lucky to have friends and colleagues like Yazgan Tuna, Ahmet Burak Cunbul, Dr. Seymur Cahangirov, Burak Gököz, Tamer Doğan, Abdulsamet Akpınar and Mite Mijalkov. I heartily thank them for their contribution to my scientific and personal growth!

Last but not least, I cannot thank enough to my mother Elif, my father Mehmet, my sisters Feride, Zeynep and her husband Richard, my brother Özgür and his wife Nursen, my sweet nephew Irem and Ayşe Yeşil for their kind and warm support throughout the years. They are all very valuable for me. Thank you!

Contents

List of Figures

Chapter 1

Introduction

Most events in nature occur on a random fashion intrinsically. Even a larger percentage of events, on the other hand, appear to be random, rather than being random per se, to an observer looking from outside to the particular system. Consequently, study of random phenomena has been very important both as a mechanism for describing the exquisite properties of nature and as a modeling tool for predicting the outcome of random events. Pointing to its importance, it can be traced back to ancient Greeks who mostly made philosophical speculations about the nature of randomness without connecting it to mathematics necessarily. Democritus (460 BC - 370 BC), who thought that all matter is made of indivisible tiny atoms, hypothesized that the whole universe is deterministic. According to his argument, randomness is related to the lack of knowledge of the human mind as there is no room for randomness in an entirely deterministic universe [1]. About 200 years later, another atomist Epicurus argued that atoms constituting the matter move randomly, so that the matter constituting the universe cannot be reduced to a pre-determined set of relations. He thought that, at the most basic level, there will always be randomness of sorts [1]. Later, in his exhaustive categories, Aristotle, according to whom all the events in the world are seperated into the categories of certain, probable and unknowable events, formulated randomness in the domain of unknowables [2].

The transition, in the study of randomness, from loose philosophical speculation to concrete mathematical formulation arrived much later than Aristotle. Incidentally, as a mathematical tool it sprung out from the need to describe the properties of physical structures at the very beginning of the last century while the work on a thorough mathematical formulation intensified with the developments in finance which heavily required better understanding of randomness. The earliest work on stochastic differential equations is Einstein's famous work on the movement of a microparticle immersed inside a fluid, which is observed by the botanist Robert Brown almost a century before Einstein [3]. Louis Bachelier, Marian Smoluchowski and Paul Langevin also contributed to the formulation of Brownian motion at the same decade. At this point, it is interesting to note that the first modeling example on the study of randomness comes from physics. A thorough mathematical formulation of the general framework of mathematics of stochastic differential equations came from the works of mathematicians Kiyoshi Itô and Ruslan Stratonovich towards the middle of the century [4, 5].

Most events in nature occur on a nonlinear fashion intrinsically as well as being random! Besides its practical importance as a modeling toolkit, nonlinearity is essential for almost all kinds of mathematical modeling on nature. It can even be argued that nature consists of randomly occuring nonlinear events more than most. Therefore, a concise and thorough understanding of the effects of random fluctuations on nonlinear systems is much needed. The work led to this thesis is aimed at the study of randomness when it is coupled with nonlinear dynamics on this ground.

In literature, it has been shown that fluctuations give rise to interesting phenomena in nonlinear systems, such as the noise-induced drift [6, 7, 8, 9, 10], Itô-Stratonovich dilemma [11, 12, 13, 14, 15] and stochastic resonance [16, 17, 18]. These effects are so useful and versatile in capturing the properties of nature that, they can be used to make predictions about the conditions on earth thousands of years ago [17] or about the information transfer in crayfish [18]. Another important aspect of these phenomena is the inherent fundamental interest related to the understanding of randomness as it has the potential for giving rise to counter-intuitive behavior such as a directed, deterministic drift borne out of the

underlying noise alone [6, 7].

This thesis starts with a lengthy introduction to the formalism of stochastic differential equations with passive and active Brownian motion as paradigmatic examples, which is followed by a short introduction on the simulation methods for stochastic differential equations. Finally, results are presented and discussed. Computational results can be classified in 3 parts: The fundamental theoretical and numerical work on the *effects of noise on nonlinear dynamics* and the applications of the results derived from this; namely, *collective behavior of microswimmers interacting with nonuniform diffusion* and *microparticle sorting with the noise-induced drift*.

The interplay between noise and nonlinear dynamics is discussed throughout the thesis. It is shown that, counter-intuitively, noise can alter the future behavior of a nonlinear system in a deterministic way despite rendering it random in the first place. The main result of this thesis is that noise changes the stochastic calculus convention with which one interprets and models a nonlinear stochastic system dynamically and deterministically depending on the underlying properties of the system. Applications of this result is studied on nonequilibrium model systems consisting of an aggregate of interacting microswimmers immersed in a heat bath and an aggregate of Brownian particles immersed in a macroscopic diffusion gradient. In both cases, interesting noise-induced effects on the collective motion of the aggregate as well as the single particle motion are observed. More precisely, it is shown that noise itself can drive particles in a given direction in such a way that this effect can be used in the realization of a particle sorter as a possible application. It is also demonstrated that, in a prey-predator system, noise can lead the system between the states of coexistence and exclusion of one species, thereby altering the stability of the system dramatically.

Chapter 2

Background

2.1 Stochastic Differential Equations

2.1.1 Drift and Diffusion

A stochastic differential equation (SDE) is formed with the addition of a term depicting randomness into an ordinary differential equation of the form

$$\frac{dX}{dt} = u(t, X_t) + D \cdot "noise"$$

where u, which comprises the deterministic part of the equation, is referred as *drift* and D, introducing randomness into the equation, is referred as *diffusion*. Under the framework of a general SDE, a rich and useful concept describing stochastic events are diffusion processes. Conceptually they are Markov processes with continuous paths.

Given that the probability of a random event taking place at time t_{n+1} is given with

$$P(X(t_{n+1})\epsilon B|X(t_1)=x_1, X(t_2)=x_2, ..., X(t_n)=x_n) \\ = \frac{\int_B p(t_1,x_1;t_2,x_2;...;t_n,x_n;t_{n+1},y)dy}{\int_{-\infty}^{\infty} p(t_1,x_1;t_2,x_2;...;t_n,x_n;t_{n+1},y)dy} \tag{2.1}$$

for all Borel subsets B of $\Re$ with time instants $0 < t_1 < t_2 < ... < t_n < t_{n+1}$ and states $x_1 < x_2 < ... < x_n \ \epsilon \ \Re$, by restricting the time dependence of this probability distrubution, the Markov property can be casted in the form:

$$P(X(t_{n+1})\epsilon B|X(t_1)=x_1, X(t_2)=x_2, ..., X(t_n)=x_n) \\ = P(X(t_{n+1})\epsilon B|X(t_n)=x_n)) \tag{2.2}$$

so that probability of the event taking place at time t_{n+1} depends only on the probability at time t_n [19]. If a series of random events satisfy the property defined in equation 2.2, the stochastic process $X(t)$ is called as a *Markov process* with transition probabilities

$$P(s,x;t,B) = P(X(t)\epsilon B|X(s)=x) \tag{2.3}$$

where $s < t$ with a transition density given by $P(s,x;t,B) = \int_B p(s,x;t,y)dy$ for all Borel subsets. If all of the transition densities of a stochastic process depend on the time difference $t-s$ only, it is referred as a homogeneous Markov processs, examples of which are the Wiener process with transition density:

$$p(s,x;t,y) = \frac{1}{\sqrt{2\pi(t-s)}} e^{-\frac{(y-x)^2}{2(t-s)}} \tag{2.4}$$

and the Ornstein-Uhlenbeck process with transition density:

$$p(s,x;t,y) = \frac{1}{\sqrt{2\pi(1-e^{-2(t-s)})}} exp(-\frac{(y-xe^{(t-s)^2})^2}{2(1-e^{-2(t-s)})}) \tag{2.5}$$

Partial derivatives of the equation 2.4 with respect to time and state yields the heat equation which, for example, describes the variation of temperature in a physical system:

$$\frac{\partial p}{\partial t} - \frac{1}{2}\frac{\partial^2 p}{\partial y^2} = 0 \tag{2.6}$$

Heat equation is a specialized case of a more general class of Kolmogorov equations which connect probability evolution with respect to time with probability evolution with respect to state. The Kolmogorov forward equation (also known as Fokker-Planck equation, especially in the physics community) gives the probability evolution with respect to time in the forward direction:

$$\frac{\partial p}{\partial t} + \frac{\partial}{\partial y}(u(t,y)p) - \frac{1}{2}\frac{\partial^2}{\partial y^2}(D^2(t,y)p) = 0 \tag{2.7}$$

whereas Kolomogorov backward equation gives that of backward in time:

$$\frac{\partial p}{\partial s} + \frac{\partial}{\partial y}(u(s,x)p) - \frac{1}{2}D^2(s,x)\frac{\partial^2 p}{\partial y^2} = 0 \tag{2.8}$$

given that drift and diffusion functions are smooth functions. Therefore, analysis of the partial derivatives of the transition probability of the Wiener process, given in 2.4, indicates of a general structure in the evolution of probability distribution of a special class of functions, named as *diffusion process* [19]. To be specific, a diffusion process is a specific form of a Markov process with the properties:

- $$lim\frac{1}{t-s}\int_{(y-x)>\epsilon} p(s,x;t,y)dy = 0 \tag{2.9}$$
- $$lim\frac{1}{t-s}\int_{(y-x)<\epsilon} (y-x)p(s,x;t,y)dy = u(s,x) \tag{2.10}$$
- $$lim\frac{1}{t-s}\int_{(y-x)<\epsilon} (y-x)^2 p(s,x;t,y)dy = D^2(s,x) \tag{2.11}$$

The first property described in equation 2.9 prevents a diffusion process from having instantenous jumps. The second property implied by 2.10 shows that:

$$u(s,x) = lim\frac{1}{t-s} < X(t) - X(s)|X(s) = x > \tag{2.12}$$

as a result of which, in a sense, the definition of drift u(s,x) becomes the instantenous rate of change in the mean of the stochastic process. In a similar fashion, the third property gives the squared diffusion coefficient as:

$$D^2(s,x) = lim\frac{1}{t-s} < (X(t) - X(s))^2|X(s) = x > \tag{2.13}$$

so that the diffusion coefficient becomes the description of the instantenous rate of change of the squared fluctuations of the stochastic process [19].

2.1.2 White Noise

The noise term in an SDE gives the correct meaning to the diffusion term by rendering the system random through the diffusion process. In order for a system to be considered random, it must have the following properties which are deducted by observation:

1. For $t_1 \neq t_2$, W_{t_1} and W_{t_2} should be independent from each other.
2. W_t should be stationary, that is, the joint probability distribution should not depend on time.
3. $< W_t > = 0$

Incidentally, the first and second properties cannot be satisfied at the same time for a given stochastic process on the grounds that such a noise function lacks continuous paths. As a result, the noise function should be interpreted as a generalized function so as to extend the notion of a function from the frameworks

of a discontinuous function into a smooth function, since smooth functions satisfy the conditions of existence and uniqueness theorem, thereby allowing many calculus operations to be applicable. Therefore, the noise function is represented as a generalized stochastic process called the white noise process, denoted by W_t [20]. White noise can be seen as the mean square derivative of a Wiener process, which is, by definition, delta-correlated in time, has zero mean and finite variance. Standard Wiener process is defined with the transition probability depicted in equation 2.4. As a result, in the general form of an SDE, randomness is introduced via the white noise, which turns into the Wiener process in the discretized form of the equation. With these properties regarding drift, diffusion and noise terms, a general stochastic differential equation can be discretized as:

$$X_{k+1} - X_k = u(t_k, X_k)\Delta t_k + \sigma(t_k, X_k)W_k\Delta t_k \tag{2.14}$$

where $X_k = X(t_k)$, $W_k = W_{t_k}$ and $\Delta t_k = t_{k+1} - t_k$. In the limit of $\Delta t_k \to 0$, this expression becomes:

$$X_t = X_0 + \int_0^t u(s, X_s)ds + \int_0^t \sigma(s, X_s)dW_s \tag{2.15}$$

As a consequence, by means of adding randomness into an ordinary differential equation through the white noise process, we model a stochastic process X_t in the form of equation 2.15.

The standard Wiener process can be modeled as a scaled random walk on any finite interval of time. By dividing the unit interval $[0, 1]$ into equal length subintervals with length $\Delta t = 1/N$ in $0 = t_0^{(N)} < t_1^{(N)} < ... < t_N^{(N)} = 1$ and adding the stipulation that the system makes a stepwise move $\sqrt{\Delta t}$ on the interval independently and with equal probabilities to either side, we can construct a random walk scheme M_N with independent increments $X_1\sqrt{\Delta t}$, $X_2\sqrt{\Delta t}$, $X_3\sqrt{\Delta t}$, ... for the given interval. Numerically, the scaled random walk M_N corresponds to

$$M_N(t_n^{(N)}) = (X_1 + X_2 + ... + X_n)\sqrt{\Delta t}$$

where X denotes the random variables which can take on values ± 1 with equal probabilities. The random walk process M_N has zero mean and a finite variance of $\Delta t[\frac{t}{\Delta t}]$ for the interval $0 \leq t \leq 1$ [20]. It follows directly from the form of M_N that $< (M_N)^2 > \rightarrow t$ as $N = 1/\Delta t \rightarrow \infty$ for any $0 \leq t \leq 1$. Hence, due to its properties of having zero mean and finite variance the requirements for Central Limit Theorem is met, so that the process M_N can be classified as standard Wiener process [20].

Existence and uniqueness theorem guarentess a unique solution under the condition that the function is both continuous and differentiable. However, as is shown, even though Wiener process is continuous, it is almost nowhere differentiable since its variance grows unboundedly with time. As a result, Wiener process is of unbounded variation with the mean always remaining at zero.

In physics and engineering applications, variance refers to the average power. In a similar fashion, the variance of a stochastic process $X(t)$ can also be interpreted in the same way:

$$< X^2(t) >= cov(0) = \int_{-\infty}^{\infty} S(w)dw \tag{2.16}$$

where cov(0) gives the covariance $cov(t-s)$ at $s = t$ and $S(w)$ describes the *spectral density* which is a measure of the average power per unit frequency at the frequency w [20]. Inverse Fourier transform of this expression gives the spectral density:

$$S(w) = \int_{-\infty}^{\infty} cov(s)cos(2\pi ws)ds \tag{2.17}$$

In a sense, spectral density of fluctuations is given by the power spectrum of the autocovariance for a random process. This is called to be the Wiener-Khinchin Theorem [21, 22]. In this respect, *Gaussian white noise* can be thought of as

a zero-mean stationary process with constant nonzero spectral density $S(w) = S_0$. As the name *white* suggests, its average power is distributed uniformly in frequency space, so it has a covariance of $cov(s) = S_0\delta(s)$ for all s.

By using delta-correlation property of white noise, we can define a new process $X^h(t)$ again with zero-mean but with a different covariance:

$$X^h(t) = \frac{W(t+h) - W(h)}{h} \tag{2.18}$$

which indicates a correlation in time with correlation length being equal to h [20]. Thus, spectral density varies depending on the value of h, a low value indicating a very broad spectrum whereas a high value for h indicates a smaller spectrum. This type of process with broad banded spectrum including correlations in time are reffered as *coloured noise processes*, an example of which is given by the Ornstein-Uhlenbeck process. Its transition probability is given in equation 2.5 and its covariance is $cov(s) = e^{-\gamma|s|}$, indicating correlations since it depends on time explicitly as opposed to the Wiener process. Comparison of equation 2.7 with 2.5 reveals that Ornstein-Uhlenbeck process can be interpreted as the stationary Markov process determined by the linear Fokker Planck equation [23].

2.1.3 Colored Noise

When the terms that make up the Langevin equation:

$$\dot{y} = U(y) + D(y)\xi(t) \tag{2.19}$$

includes a noise process $\xi(t)$ that is not white, but correlated with some finite correlation time with the given properties:

$$< \xi(t) >= 0, < \xi(t)\xi(t') >= \kappa(t - t') \tag{2.20}$$

the stationary noise process is called as a colored noise process (in which color refers to the correlations in contrast with the all-in feature of white noise process) [20]. Here the autocorrelation function κ is not a singular, delta function. Since it is correlated, the stochastic process y(t) is not a Markov process anymore. A convenient example for the colored noise process is the Ornstein-Uhlenbeck process as is described before.

2.2 Brownian Motion

Brownian motion is considered to be the paradigmatic example demonstrating the properties of stochastic differential equations. It describes the motion of a microparticle immersed in a fluid in which collision of the immersed particle with the surrounding fluid molecules cause an erratic random motion. Modeling of such motion is determined with adding a stochastic force term that captures the properties of the random motion. Essentially, the stochastic force should not cause a bias in any direction in the motion of the particle, as a result the mean of the force term should equal to zero. In addition, since the force is caused by collisions of individual fluid molecules with the particle, it should vary rapidly and each collision should be instantenous, which imply that collisions should be uncorrelated from each other. Therefore, in essence, the stochastic force term should have the properties of $< W_t >= 0$ and $< (W_t - W_{t'}) >= \Gamma\delta(t - t')$ where Γ is a constant, which match with the properties of Wiener process [24].

By Newton's second law, the equation of motion for the particle is:

$$m\dot{v} = -\gamma v + W_t \tag{2.21}$$

where the first term on the right hand side of the equation describes the damping and the second term gives the stochastic force depicting the collisions of particle with the surrounding fluid molecules. This equation describing the motion of a particle immersed in a fluid is called the Langevin equation. Its straightforward solution with treating the mass as unity yields [25]:

$$v(t) = v_0 e^{-\gamma t} + e^{-\gamma t} \int_0^t e^{-\gamma t'} W_{t'} dt \tag{2.22}$$

Taking an ensemble average, then, gives the simple equation $< v_t >= v_0 e^{-\gamma t}$ for the mean of velocity of the particle. In order to find the mean square average of the velocity, we take the square of the expression in 2.22:

$$v^2(t) = v_0^2 e^{-2\gamma t} + \Gamma e^{-2\gamma t} \int_0^t dt' \int_0^t dt'' e^{\gamma(t'+t'')} < W_{t'} W_{t''} >= v_0^2 e^{-2\gamma t} + \frac{\Gamma}{2\gamma}(1 - e^{-2\gamma t}) \tag{2.23}$$

Since as $t \to \infty$ the mean square velocity should take its thermal value, size of the fluctuations Γ is related with the damping constant γ as follows:

$$< v^2 >= \frac{\Gamma}{2\gamma} = kT \tag{2.24}$$

This simple relation is called the fluctuation-dissipation theorem as it relates the underlying fluctuations of the system with the damping in energy.

2.3 Nonlinear Stochastic Differential Equations

The modeling process in which a random motion is modeled by adding a stochastic term into the equation of motion to represent randomness is called the Langevin approach. An equivalent way to represent the same erratic motion is done with taking the partial derivatives of the probability distribution with respect to time and spatial direction which is called the Fokker Planck approach. In this sense, the Langevin equation 2.21 represents the same stochastic process as the Fokker Planck equation of [23]:

$$\frac{\partial P(v,t)}{\partial t} = v \frac{\partial}{\partial v}(vP) + \frac{\Gamma}{2} \frac{\partial^2 P}{\partial v^2} \tag{2.25}$$

The general form of a SDE under the Langevin approach becomes:

$$\dot{y} = U(y) + D(y)W(t) \tag{2.26}$$

which is equivalent to the equation under the Fokker Planck representation (which can be obtained with a few transformation of variables) [25]:

$$\frac{\partial P(y,t)}{\partial t} = -\frac{\partial}{\partial y}[U(y) + \frac{1}{2}\Gamma D(y)D'(y)]P(y,t) + \frac{\Gamma}{2}\frac{\partial^2}{\partial y^2}[D(y)]^2 P(y,t) \tag{2.27}$$

As noted before, white noise that introduces randomness into the equation of motion can be thought of as a series of delta peaks arriving at random times with zero mean and finite variance, since it is uncorrelated and is related to the change of y as a function of time. Hence equation 2.26 implies that each delta jump in the noise causes an uncorrelated, irregular change in $y(t)$, as a result the exact value of y, and therefore D(y), at the time when the delta function arrives remains undetermined. It is not specified whether the value of y into the integrand D(y) should be put before the jump, after the jump or some time in between [25]. This difference of interpretations lead to quite different Fokker Planck equations, thus to drastically different future behavior. It is important to note that mathematically there is no reason to choose one interpretation over the other; instead it is mathematically equivalent to choose either of them.

According to the Itô interpretation, the value of y before the arrival of the delta change is opted, so that the equation 2.26 becomes [25]:

$$y(t+\Delta t) - y(t) = U(y(t))\Delta t + D(y(t)) \int_t^{t+\Delta t} W(t')dt' \tag{2.28}$$

which is equivalent to the Fokker Planck equation:

$$\frac{\partial P(y,t)}{\partial t} = -\frac{\partial}{\partial y}U(y)P + \frac{\Gamma}{2}\frac{\partial^2}{\partial y^2}[D(y)]^2 P(y,t) \tag{2.29}$$

According to the Stratonovich interpretation, one should insert the mean value of y before the arrival of delta jump and after the arrival of the delta jump [25]:

$$y(t+\Delta t) - y(t) = U(y(t))\Delta t + D(\frac{y(t)+y(t+\Delta t)}{2}) \int_t^{t+\Delta t} W(t')dt' \qquad (2.30)$$

which gives the Fokker Planck equation of:

$$\frac{\partial P(y,t)}{\partial t} = -\frac{\partial}{\partial y}U(y)P + \frac{\Gamma}{2}\frac{\partial}{\partial y}D(y)\frac{\partial}{\partial y}D(y)P(y,t) \qquad (2.31)$$

2.3.1 Itô-Stratonovich Dilemma

White noise process is approximated with uncorrelated delta peaks in time which is an idealization at best in reality, because in many applications noise is usually a sharply peaked function of time with a small but finite correlation time $\tau_c > 0$. As a result, the stochastic differential equation can be considered proper without a singularity and in the limit of vanishing correlation time, $\tau_c \to 0$, it is solved with the Stratonovich interpretation of the Fokker Planck equation, according to the Wong-Zakai Theorem [26]. Stratonovich result preserves the regular transformation rules (like the chain rule) of ordinary calculus, thus one may transform the nonlinear Langevin equation into a quasilinear form. As a result, as long as the delta function is not an infinitely sharp peaked delta function, Stratonovich interpretation is employed as the more realistic choice.

When τ_c is finite, both interpretations are valid mathematically. Mathematicians, biologists and finance specialists use the Itô interpretation, because it gives conceptually simpler results on the grounds that it has the property of "not looking into the future", more precisely it's a martingale due to the fact that integrand is evaluated before the arrival of delta jump in y [25]. Itô equation is written in the form:

$$dy = U(y)dt + D(y)dW(t) \qquad (2.32)$$

Physicists, on the other hand, prefer to use the Stratonovich interpretation which reproduces some of the ordinary rules of calculus as embarked upon before. Stratonovich equation is generally written in the form:

$$dy = U(y)dt + D(y) \circ dW(t) \tag{2.33}$$

Even though different interpretations of nonlinear stochastic differential equations lead to different Fokker Planck equations, therefore to different future behavior, they can be transformed into each other with the addition or subtraction of a correction term to the drift U(t), which is usually referred as the *spurious drift* or more accurately, *noise-induced drift*.

When the randomness is introduced to an otherwise deterministic system via external noise, that is, fluctuations created with the application of a random force which has predetermined stochastic properties, Stratonovich solution is apt to be chosen since the noise is never white, but correlated with a finite time. As a result, the drift U(y) continues to determine the dynamics of the system. However, when the noise is an intrinsic property of the system itself, it is not possible to identify U(y) as the sole cause of time evolution of the system in isolation [25]. In this case, the macroscopic equations are just approximations that try to neglect the fluctuations as much as possible.

The Itô-Stratonovich dilemma arises as a result of the fact that sample paths of a Wiener process are not differentiable or of bounded variation. Even though the stochastic calculi of Itô and Stratonovich provide us mathematically valid formulations of stochastic differential equations, they leave the question of which interpretation to choose largely unanswered. From a solely mathematical point of view, both calculi are equally correct, however modeling-wise, the correct interpretation to choose, in the sense that the one that describes the future behavior of the system correctly, depends on the context of extraneous circumstances pertaining to the system. In particular, it depends on the way we interpret the white noise process (which is an idealization) to approximate the randomness inherent to the system.

2.3.2 Nonlinear Langevin Equation

To elaborate in a more mathematical and formal way, the nonlinear Langevin equation:

$$\frac{\partial y}{\partial t} = U(y) + D(y)W(t) \tag{2.34}$$

describes the motion of a Brownian particle which has a diffusion component that depends on the state of the system. Therefore, the diffusion is state-dependent and the noise is multiplicative. For such a nonuniform diffusion, the definition of the second term on the right hand side of the equation 2.34 is unclear. A generalized definition is given by the integral equation:

$$J_\alpha = D[\alpha y(t+\Delta t) + (1-\alpha)y(t)] \int_t^{t+\Delta t} dsW(s) \tag{2.35}$$

where $\alpha\epsilon[0,1]$ is a parametrization rate that reduces to the Itô convention when $\alpha = 0$, to the Stratonovich convention when $\alpha = 1/2$ and to the isothermal (or anti-Itô) convention when $\alpha = 1$. Here since $\alpha y(t+\Delta t) + (1-\alpha)y(t) = y(t) + \alpha\Delta y(t+\Delta t)$, integrating the SDE in 2.34 with equation 2.35 yields [12]:

$$\begin{aligned} y(t+\Delta t) - y(t) &= \int_t^{t+\Delta t} dsU[y(s)] + D[y(s)]W(s) \\ &= U[y(t) + \alpha\Delta y]\Delta t + D[y(t) + \alpha\Delta y] \int_t^{t+\Delta t} dsW(s) \end{aligned} \tag{2.36}$$

Combining this equation with the Taylor expansion of the diffusion term $D[y(s)] = D[y(t)] + [y(s) - y(t)]D'[y(t)]$ in the first approximation gives the mean and variance in the spatial dimension as:

$$< \Delta y >= U(y(t))\Delta t + \alpha D(y(t))D'(y(t))\Delta t \tag{2.37}$$

$$< (\Delta y)^2 >= D^2(y(t))\Delta t \tag{2.38}$$

which clearly shows the contribution of the noise-induced drift $\alpha DD'\Delta t$ to the drift term $< \Delta y >$ arising from the spatial dependence of diffusion coefficient, thus the multiplicative property of noise.

The nonlinear Langevin equation with a state-dependent diffusion describes the particle motion when there is a gradient of diffusion acting on a particle or a combination of particles. For example, for a Brownian particle diffusing near a wall, or a combination of particles immersed in a container bounded by two parallel walls exemplify the notion of motion under the effect of a diffusion gradient. For such cases, because of the intrinsic ambiguity pertaining to the definition of SDE, a correction term referred as the noise-induced drift must be added according to the interpretation one chooses in order to predict the future behavior of the noisy system correctly. The overwhelming question of which stochastic calculus solution convention or interpretation to choose depends largely on the context, an example of which is demonstrated experimently recently that sometimes underlying physics dictates the correct interpretation. In the experiment with colloidal particles immersed in a heat bath, it is shown that under the condition of thermal equilibrium, in order to get the correct future behavior of the system that is depicted in the Maxwell-Boltzmann distribution, one has to choose the anti-Itô formulation with parametrization rate α being equal to 1 [9, 10].

2.4 Active Matter

There is constant motion at the micron level whether directed or random or a combination of both. Laws of physics, namely the second law of thermodynamics, drive micro-sized particles immersed in a fluid towards thermodynamic equilibrium in which disorderliness is maximized, in the sense taht states of the system are maximized. However, even in equilibrium, microparticles move, in

an attempt to reduce their thermal energy, with a random pattern as a result of Brownian motion, namely collision of the microparticle with the surrounding particles constituting the fluid. Some microparticles, referred as microswimmers, are able to propel themselves in a fluid. Microswimmers can be classified based on how they achieve locomotion. As most of them are biological entities, they consume energy for staying out of thermodynamic equilibrium. They can also fuel their self-propulsion by manipulating their surroundings.

Most of the microswimmers have a hair-like appendage, named as flagellum, that enables locomotion by propelling the swimmer. Prokaryatoic swimmers, like the bacterium *E. coli*, have rigid, helical and passive flagella. A rotary motor on the cell wall rotates the flagellum which in turn propels the cell forward like a corkscrew turning [27]. Eukoryatic flagella, like those found on spermatozoa and certain algae, are actively deforming to achieve propulsion via molecular motors, producing bending, distributed over the flagellum itself. Collective action of these molecular motors on the flagellum induce a wave-like undulatory motion over the fluid [28]. Several eukaryotic flagella bundle together at the surface of a cell to form cilia. Cilia, like those found on algae cells, create motion by inducing power strokes due to flagella pulling in different directions [28].

The medium, in which the particles are embedded in, is a key factor for all types of motion considered. It can be characterized with the Reynolds number Re which is a measure of comparison between the inertia and viscosity, more precisely it is the ratio between inertial forces over viscous forces. Since the Reynolds number is directly proportional with the velocity and length of the swimmer and inversely proportional with the viscosity of the fluid, it is very low for swimmers that have micron sized lengths and velocities. As a result of being in a low Reynolds number regime, viscosity dominates over inertia for microswimmers. Therefore, they interact with each other over the fluid even at long distances. Depending on their effect on the fluid, microswimmers are classified in two types: Those which push the fluid in the forward direction are called to be pushers whereas the ones who pulls the fluid in front of it are referred as pullers.

Besides biological swimmers, microparticles can also propel themselves by manipulating the fluid surrounding them via making use of chemical, thermal, electromagnetic gradients. For example, Janus particles are two-faced particles with Pt-coating in one side. In a hydrogen peroxide solution, when they are heated the Pt-coated side starts to react with the H_2O_2 solution, thereby a chemical gradient is induced over the fluid over which particle can be propelled [29].

Chapter 3

Simulation

3.1 Euler-Maruyama Method

Simulation process, in essence, consists of mimicking the properties of a given system so as to understand and possibly predict its future behavior. Numerical models of stochastic differential equations, which model systems including randomness, are essential for this end. For modeling the evolution of a regular system without any randomness, one of the most common ways is the finite difference simulation of an ordinary differential equation that describes the system. Within the frameworks of the finite difference method (also known as Euler method), continuous time solution $x(t)$ of an ODE is approximated with a discrete time sequence x_i. The ODE is discretized with time steps $t_i = i\Delta t$ and in the limit of $\Delta t \to 0$, the time derivative of the continuous process $\dot{x}(t)$ can be approximated with:

$$\dot{x}(t) = \frac{x_i - x_{i-1}}{\Delta t} \tag{3.1}$$

Consequently, the second derivative with respect to time becomes:

$$\ddot{x}(t) = \frac{(x_i - x_{i-1})/\Delta t - (x_{i-1} - x_{i-2})/\Delta t}{\Delta t} = \frac{x_i - 2x_{i-1} + x_{i-2}}{\Delta t^2} \tag{3.2}$$

The solution is obtained by solving the resulting finite difference equation recursively for x_i with the values from previous iterations x_{i-1} and x_{i-2}. Euler-Maruyama method is the extension of Euler method of ordinary differential equations to stochastic differential equations. The key to going from ODEs to SDEs is the simulation of noise, that is the simulation of randomness per se.

3.1.1 White Noise

White noise process W_t is determined with the properties of having zero mean, finite variance and being uncorrelated in time, so that W_{t_1} and W_{t_2} are independent from each other for $t_1 \neq t_2$. Since it is nowhere differentiable as a result of these properties and its being of unbounded variation, it cannot be approximated with its instantenous values at given times. Given the fact that white noise process is at the core of stochastic simulations, it is of utmost importance to turn to numerical recipes, namely discretization of random intervals that mimic the behavior of W_t. Therefore, the discretized random interval W_i should consist of uncorrelated random numbers with zero mean and variance $\frac{1}{\Delta t}$, so that we impose the condition:

$$\frac{< (W_i \Delta t)^2 >}{\Delta t} = 1 \tag{3.3}$$

Since this random number sequence is uniquely determined with is mean and variance, we should generate a Gaussian random number sequence between the values 0 and 1 and then rescale with multiplying the sequence with $1/\sqrt{\Delta t}$, so that it will have the correct variance [30].

3.1.2 Random Walk

1-D random walk is the paradigmatic example demonstrating the simulation of white noise with the Euler-Maruyama method. In a very straightforward fashion, its motion is described with the simple SDE:

$$\dot{x}(t) = W(t) \tag{3.4}$$

which, within the finite difference approximation, turns into:

$$\frac{x_i - x_{i-1}}{\Delta t} = \frac{w_i}{\sqrt{\Delta t}} \tag{3.5}$$

that is equivalent to:

$$x_i = x_{i-1} + \sqrt{\Delta t} w_i \tag{3.6}$$

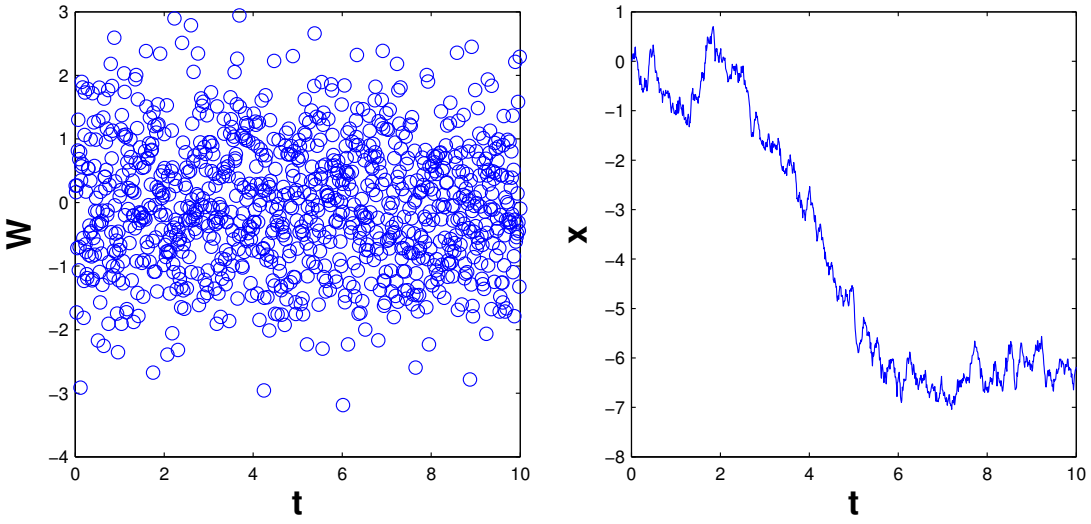

Figure 3.1: Random number sequence and the corresponding sample path of free diffusion as a function of time with $dt = 0.01$ and $N = 100$. The code is given in Appendix B.1.

where w_i is a stationary Gaussian random number sequence in the interval $[0, 1]$ with zero mean and finite variance [30]. Since there is no characteristic time scale for a case without diffusion, there is no constraint in the simulation time step. As a result, it is straightforward to simulate a 1-D random walk process with free diffusion.

3.1.3 Colored Noise

The main difference between the white noise process and the colored noise process is related to the fact the colored noise process involves correlations in time as opposed to the white noise process, so that the process $C(t_1)$ is not independent from $C(t_2)$ for $t_1 \neq t_2$ which implies the existence of a memory kernel of sorts in the system. A common example demonstrating the properties of the colored noise is the Ornstein-Uhlenbeck process [31, 32]. Like the white noise proces, it is a stationary Gaussian process, therefore it can be described with a mean and a variance. It is of bounded variation and it has a drift value that is not constant in contrast with the white noise process; instead the system evolves towards a long-term mean value taking on positive and negative values depending on the relation between the drift value at a given time and the long-term mean value. As a result, it is referred as a mean-reverting process [33].

Because of its mean-reverting property, it can describe the evolution of a Hookean spring subject to thermal fluctuations that changes its length on a random basis. It can be written as a stochastic differential equation in the Langevin form:

$$\gamma \dot{x}(t) = -k(x(t) - x_0) + \xi(t) \tag{3.7}$$

We generate colored noise random number sequence by means of Ornstein-Uhlenbeck process that is exponentially correlated in time explicitly, so it has an exponential memory kernel. One thing to note when simulating colored noise is that the correlation time τ should be larger than the simulation time step dt in

order to prevent a logical mistake numerically.

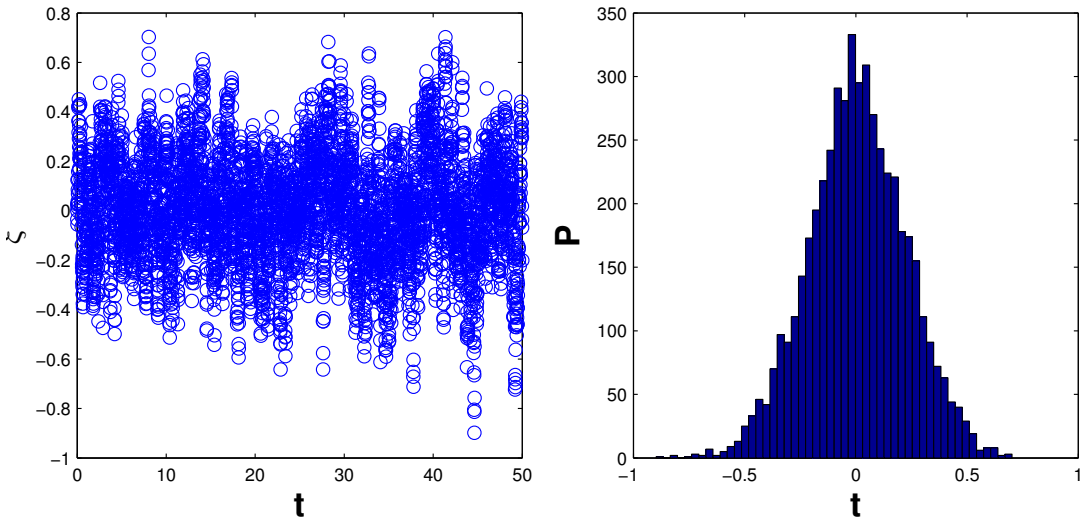

Figure 3.2: Random number sequence and the corresponding probability distribution of Ornstein-Uhlenbeck process with time step $dt = 0.01$ and correlation time $\tau = 0.1$. As depicted, probability distribution of random numbers shows a pronunced Gaussian distribution. The code is provided in Appendix B.2.

In the limit of vanishingly small correlations, $\tau \to 0$, stochastic process resembles the white noise process more and more. In the case of multiplicative noise, it is expected, by Wong-Zakai theorem, that in the same limit the correct stochastic approximation is given by the Stratonovich interpretation with the parametrization rate $\alpha = 0.5$ [34].

3.2 Monte Carlo Simulations

In essence, a Monte Carlo simulation consists of suggesting trial moves based on random numbers to a system and then checking if the suggested move holds or not depending on a set of deterministic constraints [35]. We use a Monte Carlo algortihm to calculate the evolution of an aggregate of microswimmers immersed

in a fluid. Our model consists of active spherical microparticles immersed in water. Microswimmers affect a fluid by changing its viscous properties locally which is modeled with a change in diffusion coefficient via the fluctuation-dissipation theorem that relates the fluctuations in the fluid (diffusion) with the dissipation in energy (damping). Therefore, affect of each microswimmer on the fluid is approximated with a diffusion gradient as depicted in Fig. 4.5. To make things more realistic, the induced diffusion gradient is repulsive at short scales, which corresponds to a low diffusion coefficient and attractive at longer distances from the center of the particle corresponding to a high diffusion coefficient. In fact, diffusion coefficient doesn't cause attraction or repulsion per se, since it is multiplied with a noise term in the Langevin equation that randomizes the diffusion process. However, in the case of a nonuniform diffusion, the noise-induced drift which is not multiplied with noise can lead to such effects. Therefore, in order to account for these effects, we introduce a diffusion gradient in the form:

$$D = D_C + \frac{A}{w\sqrt{2\pi}} e^{-\frac{r^2}{2w^2}} [(x - x_p - s_x cos(\phi))cos(\phi) + (y - y_p - s_y sin(\phi))sin(\phi)] \quad (3.8)$$

where (x, y) is the position where the diffusion is evaluated, (x_p, y_p) gives the coordinates of the current particle position, (s_x, s_y) is the shift in the diffusion coefficient calculation, ϕ is the angle between the center of the particle and the point where the diffusion is evaluated and A and w being normalization constants. Partial derivatives of the diffusion function with respect to x and y yield the noise-induced drifts in x and y directions.

We put all of the microparticles inside a square box, filled with water, with length $L = c + 2RN$ where R is the radius of the particle, N is the number of particles and c is a parameter that defines the confinement of the particles. We apply periodic boundary conditions in order to get rid of unwanted surface effects. Initial position of the particles are chosen randomly and the first step in the algorithm consists of calculating the initial diffusion coefficients and noise-induced drifts based on this random initial distribution. Then, by employing the

rotational Langevin equation

$$\phi_{n+1} = \phi_n + \sqrt{2D_r dt}W$$

and Langevin equations in the translational directions x and y

$$\begin{aligned} x_{n+1} &= x_n + \sqrt{2D_t(x,y)dt}W + \alpha\frac{\partial D(x,y)}{\partial x}dt + vcos(\phi) \\ y_{n+1} &= y_n + \sqrt{2D_t(x,y)dt}W + \alpha\frac{\partial D(x,y)}{\partial y}dt + vsin(\phi) \end{aligned} \tag{3.9}$$

a trial movement is suggested for each particle (the stochastic calculus parameter α is chosen to be 1 -depicting anti-Itô characteristics- since we assume thermodynamic equilibrium). Within the algorithm, since particles are modeled as hard spheres, particle positions after the suggested trial moves are checked to see if there is any collision between the particles. In the case of a collision, the suggested move is taken back completely and thereby the initial particle position is sustained. However, if there are no collisions, the move is allowed, so the particles move inside the box accordingly with the periodic boundary conditions. After that, diffusion coefficients and noise-induced drifts are calculated again for each particle at their newly acquired respective position and the whole process of suggesting a trial move based on Langevin equations, checking for collisions repeats on and on until the simulation step size is reached. The code for the simulation is provided in the Appendix.

Chapter 4

Results

4.1 Effects of Noise on Nonlinear Dynamics

4.1.1 Stratonovich-to-Itô Transitions in Lotka Volterra Model with Symmetric Competition

The Lotka-Volterra Model is an ecological model that describes the evolution of prey-predator populations in an environment. It is originally introduced by Vito Volterra to explain the unexpected increase of shark population during World War I [36]. The model itself is interesting from a fundamental point of view, besides serving as a description for ecological phenomena, as a result of nonlinearities embedded in its formulation.

In addition to the nonlinearity, an environment is often subject to noise, therefore in order to develop a real understanding of prey-predator dynamics, adding noise and time delay is more than essential [37]. Although the deterministic equations have been studied heavily over the years, study of effects of noise and time delay on the nonlinearities intrinsic to the system had begun relatively recently [38, 39, 40]. Noise-induced phenomena such as stochastic resonance, spatio-temporal patterns and delay induced phenomena pertaining to the model

have been demonstrated [41, 42, 43, 44].

In systems involving multiplicative noise, there is an ambiguity in the choice of stochastic solution convention that results in the alteration of the temporal behavior of the system in quite an important way. The intrinsic ambiguity rooted in the very definition on the choice of stochastic conventions is often overlooked in the literature to our knowledge, because it is relatively hard to observe the differences between different solution conventions qualitatively. Here, we demonstrate that different conventions predict quite different future behavior for the parameters, in the case of Lotka-Volterra, for the evolution of population of the interacting species. We also show that the choice on stochastic calculus convention depends entirely on the underlying dynamics of the system, we pin this down to the delay time in the feedback giving rise to the nonlinearity. Our system can be generalized to any mathematical relation involving multiplicative noise. The proposed model can be applied to actual population dynamics in nature as feedback delay time can be thought of as the time it takes for a species to join the interaction between the populations.

Competitive Lotka Volterra model describes the competition of two species in the same environment for the same resource. It stipulates that, $\frac{dx}{dt}$ and $\frac{dy}{dt}$ are decreasing functions of both x *(intraspecific competition)* and y *(interspecific competition)* [45]. Hence, the symmetric set of equations in 2 dimensions are given with:

$$\begin{aligned} \frac{dx}{dt} &= ax(1 - x - by) \\ \frac{dy}{dt} &= ay(1 - y - bx) \end{aligned} \tag{4.1}$$

where a is the intrinsic growth rate of the species and b is the interaction parameter between the two species.

We propose a closed system with two competing species. Ecologically, feedback delay time is the time it takes for one species to grow from the egg state to the adult state. In our system, while one species have a low feedback delay

time (e.g., a butterfly that becomes adult rather fast), in opposition, the other one have a high feedback delay time (e.g., a hummingbird which becomes adult slowly when compared with the butterfly and it feeds with the same resources as the butterfly).

For the deterministic system in which there is no noise, there are stationary points in 2 and 3 dimensions by the Poincaré-Bendixson theorem [46]. In order to find the steady state values, time rate of change of both populations are set equal to 0:

$$\begin{aligned} 1 - x - by &= 0 \\ 1 - y - bx &= 0 \end{aligned} \tag{4.2}$$

which reveal 4 different steady state solutions, 3 of which are trivial in the sense that they are independent of the value of b. Stability of these steady state solutions are determined by the trace and the determinant of the corresponding Jacobi matrices for each point.

$$J = \begin{pmatrix} a - 2ax - aby & -abx \\ -aby & a - 2ay - abx \end{pmatrix}$$

For the point (0,0); both trace and determinant of J([0,0]) are positive, as a result the solution is not stable. Hence, this point is excluded in the temporal behaviour of populations.

For the points (1,0) and (0,1) in which one population extinguishes while the other one survives, trace of Jacobi matrices are negative and determinants are equal to 0. As a result, these points are both stable and act as centers.

In the case of b=1, the non-trivial point is determined by the line $x + y = 1$. For this point, sign of the interaction parameter characterizes the future behavior of the system [47]. For symmetric competing species, sign and value of the corresponding interaction parameters are fixed but when the symmetry breaks between

the two equations as a result of noise, stability criteria changes accordingly with the sign of the interaction parameter.

Gaussian white noise is incorporated into the equation as follows:

$$\begin{aligned} \frac{dx}{dt} &= ax(1-x-by) + \sigma x dW_x + \alpha\sigma^2 x \\ \frac{dy}{dt} &= ay(1-y-bx) + \sigma y dW_y + \alpha\sigma^2 y \end{aligned} \tag{4.3}$$

where σ is the noise intensity and $\alpha \, \epsilon \, [0, 1]$ is a parameter that determines which stochastic calculus convention would be used.

In the case both populations are Itô or Stratonovich, noise becomes too large to observe any qualitative transition, since the system becomes completely randomized because of large noise (see Fig. 4.1). For both situations, noise induces anti-correlated, quasi-periodic oscillations of both populations and there is coexistence between the two species. However, when behavior of one of the species is different, future outcome of population dynamics changes dramatically.

In the case that populations follow different stochastic calculus solution convention rules from each other, future behavior of the system changes due to the fact that in equation 4.3, x and y will take different α values which will result in different drift values that may increase one population more than the other. As a result, in the case of one population obeying Itô calculus and the other one obeying Stratonovich calculus, population that shows Stratonovich characteristics may dominate over the other species, so that one species becomes extinct. The reason behind this transition from coexistence to extinction lies in the fact that Stratonovich calculus requires $\alpha = 0.5$ which is larger than the Itô value of $\alpha = 0$, therefore stability of the system changes in favour of the Stratonovich population, that is, equilibrium point of the system is altered towards the dominance of Stratonovich population [48].

Correlated colored noise with a delay in the feedback function is introduced like this:

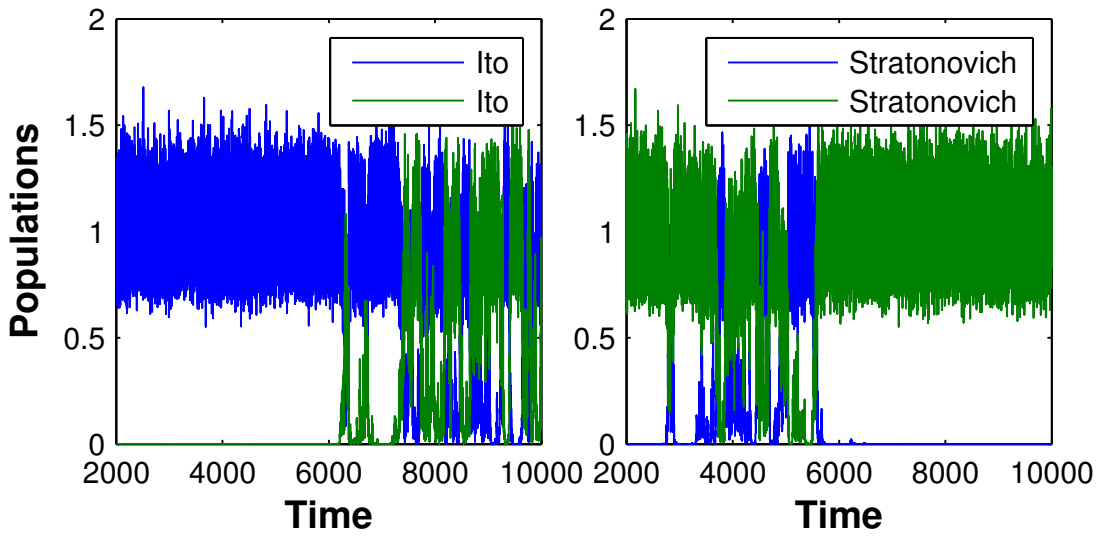

Figure 4.1: When both parameters display Itô or Stratonovich characteristics, noise becomes too large to induce a difference between the cases where both parameters are Itô and both parameters are Stratonovich. As can be seen, there are anti-correlated, quasi-periodic oscillations for both parameters after the initial transients dies out.

$$\begin{aligned} \frac{dx}{dt} &= ax(1-x-by) + \sigma x(t-\delta) \\ \frac{dy}{dt} &= ay(1-y-bx) + \sigma y(t-\delta) \end{aligned} \tag{4.4}$$

It is well known that, by the Wong-Zakai theorem, a system with white noise should be approximated with the Stratonovich solution [34]. If colored noise is used instead of white noise, when correlation time is decreased, since colored noise would behave more like the white noise as a result of decreased correlation, it is expected at first glance that the system should resemble more the Stratonovich convention. However, we report that it is not the case in systems which include multiplicative noise. As a result of the interplay between the feedback delay time and the correlation time, as correlation time gets smaller, the system makes a transition from Stratonovich convention to the Itô convention which is manifested in extinction of the species having the Itô convention. The intricate reason behind these transitions is related to the martingale property of Itô convention which

gives it the so-called "not looking into the future" behavior. Correspondingly when delay time in the feedback is increased, the system loses information, that is, it loses its memory, thereby mimicking the martingale property of Itô convention. As a result, high feedback delay time in a system corresponds to Itô convention whereas that of low feedback delay time is the Stratonovich convention in unison with the Wong-Zakai theorem [15].

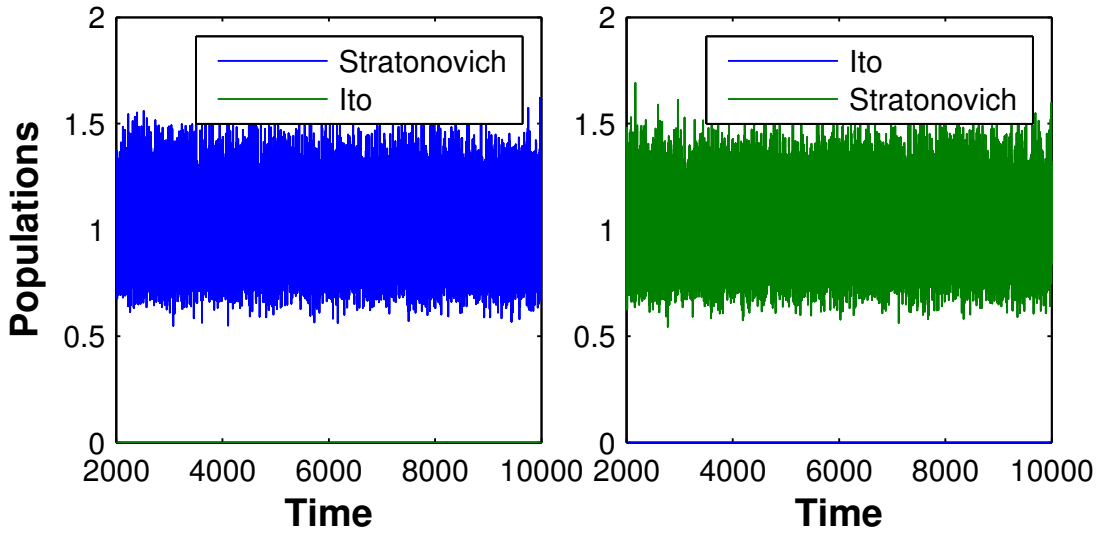

Figure 4.2: The species showing the characteristics of Stratonovich convention (*i.e.*, having a low feedback delay time such as butterflies compared with hummingbirds) wins the competition by dominating over the species with Itô characteristics (a species with a high feedback delay time such as hummingbirds when compared with butterflies).

Stratonovich-to-Itô transitions must be taken into account in the modeling of stochastic systems that show nonlinear properties. The intrinsic mathematical ambiguity, originating from the introduction of randomness into the system in the first place, is overcome with determining how the integrand in the corresponding SDE is defined deterministically by relating it to the underlying dynamics of the system. Namely, the parametrization value α, which indicates the stochastic calculus solution convention, is related to the ratio between the correlation time of the noise over the feedback delay time, δ/τ, thereby the solution convention becomes pre-determined rather than being chosen random [48, 15].

4.1.2 An SDE Approximation for Stochastic Differential Delay Equations with Colored State-Dependent Noise

It is often natural to introduce a delay into a stochastic differential equation to account for the fact that the system's response to changes in its environment is not instantenous. We are, therefore, led to consider stochastic differential delay equations (SDDEs). While there exists a general theory of SDDEs, it is much less developed and explicit than the theory of SDEs. It is thus useful to develop working approximations of SDDEs by SDEs. We derived an approximation of SDDEs driven by colored noise (or noises) in which the correlation time of the noise is of the same order as the response delay (or delays).

We consider the general multidimensional system:

$$dx_t = f(x_t)dt + g(x_{t-\delta})\eta_t dt \tag{4.5}$$

where $x_t = (x_t^1, ..., x_t^i, ..., x_t^m)^T$ is the state vector, $f(x_t) = (f^1(x_t), ..., f^i(x_t), ..., f^m(x_t))^T$ where f is a vector-valued function describing the deterministic part of the dynamical system,

$$g(x_{t-\delta}) = \begin{pmatrix} g^{11}(x_{t-\delta}) & \cdots & g^{1j}(x_{t-\delta}) & \cdots & g^{1n}(x_{t-\delta}) \\ \vdots & \ddots & \vdots & \ddots & \vdots \\ g^{i1}(x_{t-\delta}) & \cdots & g^{ii}(x_{t-\delta}) & \cdots & g^{in}(x_{t-\delta}) \\ \vdots & \ddots & \vdots & \ddots & \vdots \\ g^{m1}(x_{t-\delta}) & \cdots & g^{mi}(x_{t-\delta}) & \cdots & g^{mn}(x_{t-\delta}) \end{pmatrix}$$

where g is a matrix-valued function $x_{t-\delta} = (x^1_{t-\delta_1}, ...x^i_{t-\delta_i}, ...x^m_{t-\delta_m})^T$ is the delayed state vector (note that each component is delayed by an independent amount $\delta_i > 0$), and $\eta_t = (\eta_t^1, ..., \eta_t^j, ...\eta_t^n)^T$ is a vector of independent noises η^j, where η^j are colored (harmonic) noises with characteristic correlation times τ_j. These stochastic processes have continuously differentiable realizations which makes the

realizations of the solution process x_t twice continously differentiable.

Equation 4.5 is written componentwise as:

$$\frac{dx^i(t)}{dt} = f^i(x^1(t),\ \ldots\ , x^m(t)) + \sum_{j=1}^{n} g^{ij}(x^1(t-\delta_1),\ \ldots\ , x^m(t-\delta_m))\eta^j(t) \quad (4.6)$$

We define the process $y^i(t) = x^i(t-\delta_i)$. In terms of the y variables, equation 4.6 becomes:

$$\frac{dy^i(t+\delta_i)}{dt} = f^i(y^1(t+\delta_1),\ \ldots\ , y^m(t+\delta_m)) + \sum_{j=1}^{n} g^{ij}(y^1(t),\ \ldots\ , y^m(t))\eta^j(t) \quad (4.7)$$

Expanding to first order in δ_i, we have $\dot{y}^i(t+\delta_i) \cong \dot{y}^i(t) + \delta_i \ddot{y}^i(t)$ and

$$f^i(y^1(t+\delta_1),\ \ldots\ , y^m(t+\delta_m)) \cong f^i(y^1(t),\ \ldots\ , y^m(t)) + \sum_{k=1}^{m} \delta_k \frac{\partial f^i(y^1(t),\ \ldots\ , y^m(t))}{\partial y_k} \frac{dy^k(t)}{dt}$$

Substituting these approximations into equation 4.7, we obtain a new (approximate) system:

$$\frac{dy^i(t)}{dt} + \delta_i \frac{d^2y^i(t)}{dt^2} = f^i(\mathbf{y}(t)) + \sum_{k=1}^{m} \delta_k \frac{\partial f^i(\mathbf{y}(t))}{\partial y_k} \frac{dy^k(t)}{dt} + \sum_{j=1}^{n} g^{ij}(\mathbf{y}(t))\eta^j(t)$$

where $\mathbf{y}(t) = (y^1(t),\ \ldots\ , y^m(t))^{\mathrm{T}}$. We write these equations as the first order system:

$$\begin{cases} dy_t^i &= v_t^i dt \\ dv_t^i &= \left[-\frac{1}{\delta_i} v_t^i + \frac{1}{\delta_i} f^i(\mathbf{y}_t) + \frac{1}{\delta_i} \sum_{k=1}^{m} \delta_k \frac{\partial f^i(\mathbf{y}_t)}{\partial y_k} v_t^k + \frac{1}{\delta_i} \sum_{j=1}^{n} g^{ij}(\mathbf{y}_t)\eta_t^j \right] dt \end{cases} \quad (4.8)$$

We study the limit of the system 4.5 as the time delays δ_i and the correlation times of the colored noises go to zero. We take each colored noise η^j to be a harmonic noise process which is defined as the stationary solution of the SDE:

$$\begin{cases} d\eta_t^j &= \frac{1}{\tau_j}\frac{\Gamma}{\Omega^2} z_t^j dt \\ dz_t^j &= -\frac{1}{\tau_j}\frac{\Gamma^2}{\Omega^2} z_t^j dt - \frac{1}{\tau_j}\Gamma \eta_t^j dt + \frac{1}{\tau_j}\Gamma dW_t^j \end{cases} \tag{4.9}$$

where $\Gamma > 0$ and Ω are constants, $W_t = (W_t^1, ..., W_t^j, ..., W_t^n)^T$ is an n-dimensional Wiener process, and τ_j is the correlation time of the Ornstein-Uhlenbeck process obtained by taking the limit Γ, $\Omega^2 \to \infty$ while keeping $\frac{\Gamma}{\Omega^2}$ constant. As $\tau_j \to 0$, η_t^j converges to a white noise process. Supplemented by these equations defining the noise processes η^j, equations 4.8 become the SDE system we study. We assume that the delay times δ_i and the noise correlation times τ_j are proportional to a single characteristic time ϵ, i.e. $\delta_i = c_i\epsilon$ and $\tau_j = k_j\epsilon$ where $c_i, k_j > 0$ remain constant in the limit $\delta_i, \tau_j, \epsilon \to 0$.

If we consider f^i as functions with bounded continuous derivatives and bounded second derivatives and that the g^{ij} are functions with bounded continuous first derivatives, let $(y_t^\epsilon, v_t^\epsilon, \eta_t^\epsilon, z_t^\epsilon)$ solve equations 4.5 and 4.9 (which depend on ϵ through δ_i, τ_j) with initial conditions (y_0, v_0, η_0, z_0) the same for every ϵ (where (η_0, z_0) are distributed according to the stationary distribution corresponding to equation 4.9). Let also that y_t solves the equation:

$$\begin{aligned} dy_t^i = f^i(y_t)dt + \sum_{p,j} g^{pj}(y_t)\frac{\partial}{\partial y_p}(g^{ij}(y_t))\left[\frac{k_j(c_p\Gamma^2 + k_j\Omega^2 - c_p\Omega^2)}{2(c_p^2\Gamma^2 + c_pk_j\Gamma^2 + k_j^2\Omega^2)}\right] \\ + \sum_j g^{ij}(y_t)dW_t^j \end{aligned} \tag{4.10}$$

with the same initial condition y_0. Then taking the limit $\Gamma, \Omega^2 \to \infty$ in equation 4.10 while keeping $\frac{\Gamma}{\Omega^2}$ constant, we get the simpler limiting equation:

$$dy_t^i = f^i(y_t)dt + \sum_{p,j} g^{pj}(y_t)\frac{\partial}{\partial y_p}(g^{ij}(y_t))\frac{1}{2}\left(1+\frac{\delta_p}{\tau_j}\right)^{-1} + \sum_j g^{ij}(y_t)dW_t^j \quad (4.11)$$

which, essentially, is an equation without a colored noise term. Therefore, the main result reduces the system of stochastic differential delay equations 4.5 to a simpler system (equations 4.10 and 4.11). First we use Taylor expansion to obtain the (approximate) system of SDEs 4.8 and then we further simplify it by taking the limit as the time delays and correlation times of the noises go to zero. This is useful for applications as the final equations are easier to analyze than the original ones.

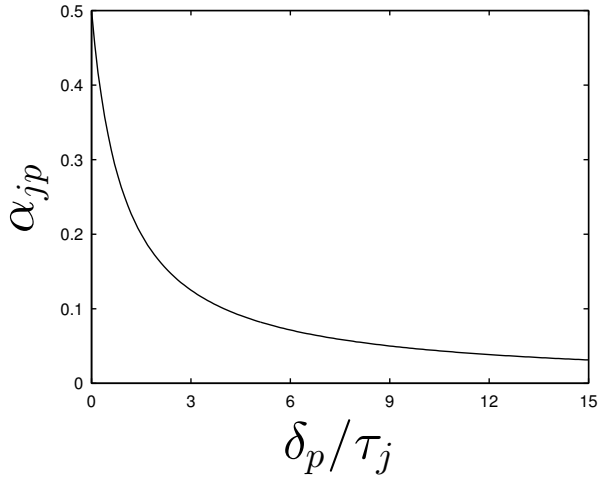

Figure 4.3: Dependence of the coefficients α_{jp} of the noise-induced drift on the ratio between the corresponding delay time δ_p and noise correlation time τ_j (see equation 4.13). For $\delta_p/\tau_j \to 0$, the solution converges to the Stratonovich integral of equation 4.14, while, for $\delta_p/\tau_j \to \infty$, the solution converges to its Itô integral.

Equations 4.10 and 4.11 also reveal the correct way to interpret the stochastic integrals in the limiting SDE in terms of the ratios of the time delays to the correlation times in the physical system. In fact, for a stochastic integral $\int_0^T g(y_t) \circ_\alpha dW_t \equiv \lim_{N\to\infty}\sum_{n=0}^{N-1} g(y_{t_n})\Delta W_{t_n}$, where $t_n = \frac{n+\alpha}{N}T$ and $\alpha \in [0,1]$, different choices of α may lead to different values of the integral [24] because W_t does not have finite variation. Common choices are the *Itô integral* with $\alpha = 0$ [4] and the *Stratonovich integral* with $\alpha = 0.5$ [5], while also the choice $\alpha = 1$ has

been shown to naturally emerge for systems in equilibrium with a heat bath [9]. Since different choices for α may lead to dramatically different qualitative behavior of the system [15], a complete model is only determined when the convention, i.e., the value of α, with which to interpret the stochastic integral is determined [11]. The ambiguity in the interpretation of the stochastic integral can be taken out of the construction of the integral itself and placed in an additional (noise-induced) drift term whose coefficient is the value of α used in constructing the original stochastic integral. That is, we have

$$\int_0^T g(y_t) \circ_\alpha dW_t = \int_0^T \alpha g'(y_t) g(y_t) dt + \int_0^T g(y_t) dW_t$$

where the stochastic integral on the right is interpreted in the Itô ($\alpha = 0$) sense. The above formula is generalized to the multidimensional case as follows:

$$\int_0^T (g(y_t) \circ_\alpha dW_t)_i = \sum_{p,j} \int_0^T \alpha_{jp} g^{pj}(y_t) \frac{\partial g^{ij}(y_t)}{\partial y_p} dt + \int_0^T (g(y_t) dW_t)_i$$

where the stochastic integral on the right is interpreted in the Itô sense.

As a result of dependence of the noise coefficients on the state of the system (multiplicative noise), a *noise-induced drift* appears in equation 4.10. It has a form analogous to that of the *Stratonovich correction* to the Itô equation with the noise term $\sum_j g^{ij}(y_t) dW_t^j$. Each drift is a linear combination of the terms $g^{pj}(y_t) \frac{\partial}{\partial y_p}(g^{ij}(y_t))$, but, while in the Stratonovich correction they all enter with coefficients equal to $\frac{1}{2}$, their coefficients in the additional drift of the limiting equation 4.10 are:

$$\frac{k_j(c_p\Gamma^2 + k_j\Omega^2 - c_p\Omega^2)}{2(c_p^2\Gamma^2 + c_p k_j \Gamma^2 + k_j^2\Omega^2)}. \tag{4.12}$$

These coefficients approach their limiting value:

$$\alpha_{jp} = \frac{1}{2}\left(1 + \frac{\delta_p}{\tau_j}\right)^{-1}, \tag{4.13}$$

as the harmonic noise approaches the Ornstein-Uhlenbeck process, i.e. taking the limit $\Gamma, \Omega^2 \to \infty$ while keeping $\frac{\Gamma}{\Omega^2}$ constant (see Fig. 4.3). One can interpret the

terms of the noise-induced drift as representing different stochastic integration conventions. For example, if all $\delta_p/\tau_j \to 0$, the solution converges to the Stratonovich integral of

$$dy_t^i = f^i(y_t)dt + \sum_j g^{ij}(y_t)dW_t^j, \tag{4.14}$$

which is equation 4.10 without the noise-induced drift terms; if all $\delta_p/\tau_j \to \infty$, the solution converges to the Itô integral of the above equation.

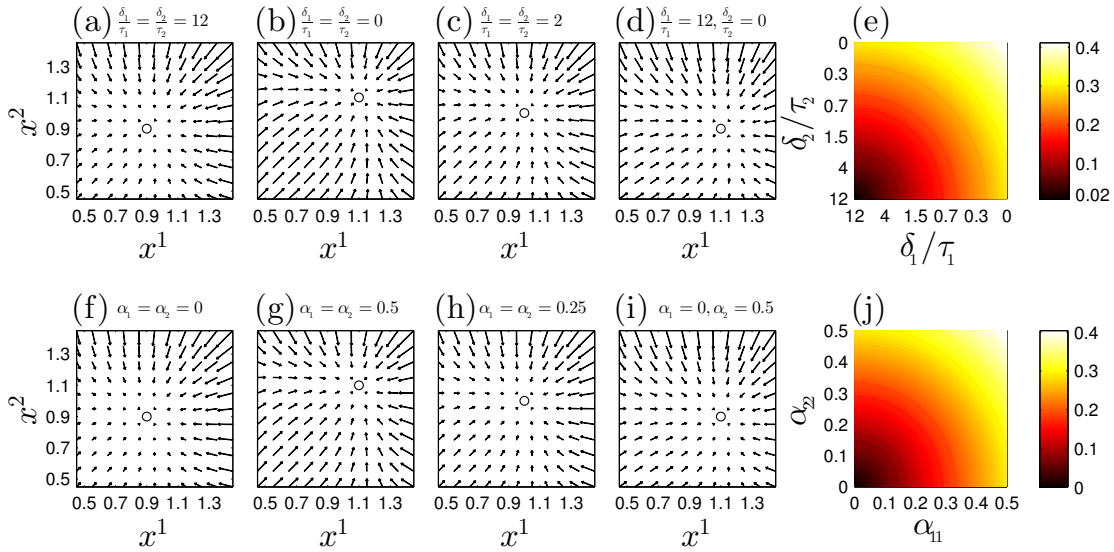

Figure 4.4: (a-d) Drift fields (arrows) estimated from a numerical solution of the SDDEs 4.15 with colored noises ($A = B = 0.1$ and $\sigma = 0.2$) for various values of the ratios δ_1/τ_1 and δ_2/τ_2. The circles represent the zero-drift points. (e) Modulus of the displacement of the zero-drift point from the equilibrium position corresponding to equations 4.15 without noise ($\sigma = 0$) as a function of δ_1/τ_1 and δ_2/τ_2. (f-i) Drift fields (arrows) of the solution of the limiting SDEs 4.11 corresponding to the SDDEs 4.15. α_{11} and α_{22} are given as functions of δ_1/τ_1 and δ_2/τ_2 by equation 4.13. The circles represent the zero-drift points. There is good agreement between (f-i) and (a-d). (j) Modulus of the displacement of the zero-drift point from the equilibrium position corresponding to equations 4.15 without noise ($\sigma = 0$) for the solution of the limiting SDEs 4.11 corresponding to the SDDEs 4.15 as a function of α_{11} and α_{22}. Again, (j) and (e) are in good agreement.

While convergence of equations 4.8 to 4.11 is rigorously shown, a specific system with non-zero values of δ_p and τ_j is more accurately described by 4.8 than

by 4.11. In addition equations 4.8 were obtained from the original system 4.5 by an approximation (Taylor expansion). It is thus important to compare the behavior of the numerical solutions of 4.8 and 4.11 in a particular case. As an example, we consider the two-dimensional system:

$$\begin{cases} dx_t^1 &= A\,x_t^1\,(1 - x_t^1 - B\,x_t^2)\,dt + \sigma\,x_{t-\delta_1}^1\,\eta_t^1\,dt \\ dx_t^2 &= A\,x_t^2\,(1 - x_t^2 - B\,x_t^1)\,dt + \sigma\,x_{t-\delta_2}^2\,\eta_t^2\,dt \end{cases} \tag{4.15}$$

where A, B and σ are non-negative constants, η_t^1 and η_t^1 are colored noises with correlation times τ_1 and τ_2 respectively and δ_1 and δ_2 are the delay times. These equations can describe, e.g. the dynamics of a noisy ecosystem where two populations are present whose sizes are proportional to the state variables x_1 and x_2. In the absence of noise ($\sigma = 0$) the system described by equations 4.15 is known as the competitive Lotka-Volterra model [45] and has only one stable fixed point at $x_{\text{eq}}^1 = x_{\text{eq}}^2 = (1 + B)^{-1}$ for which $x_{\text{eq}}^1, x_{\text{eq}}^2 \neq 0$. For a noisy system (with or without delay) there are no fixed points. One can still resort to an estimation of the system's drift field and identify the points in the state space where the drift is zero. For the system described by equations 4.15, the drift fields and the coordinates of the zero-drift point (for which $x_{\text{eq}}^1, x_{\text{eq}}^2 \neq 0$) depend on δ_1/τ_1 and δ_2/τ_2, as shown in Figs. 4.4(a-e) for $A = B = 0.1$ and $\sigma = 0.2$. We now calculate the drift fields and fixed points of the corresponding limiting SDEs 4.11. The results, shown in Figs. 4.4(f-j), are in good agreement with the ones obtained by directly simulating equation 4.15.

In conclusion, the main result shows how the underlying dynamics of a system that can be described by the means of SDDEs determine the correct integration conventions for the approximating SDEs; in particular, by determining the ratio of the time delay to the correlation time in the system, one can determine the correct way to interpret the stochastic integral. This also implies that, if the experimental or operational conditions of a single physical system are changing, then the correct interpretation of the stochastic integral may also be changing.

4.2 Collective Behavior of Microswimmers Interacting with Nonuniform Diffusion

We study the collective behavior of microswimmers interacting through nonuniform gradients of diffusion induced by themselves. Each particle creates a diffusion gradient, consistent with thermodynamical equilibrium conditions, that affects the other particles in such a way that depending on the confinement of particles anomalous diffusion is observed. When the Langevin equation, which describes the equation of motion for a Brownian particle, contains a multiplicative noise term, such as for particles under confinement as is the case in our model, an extra drift term proportional with the gradient of diffusion appears in the equation. In our model, the action of the noise-induced drift, combined with the diffusion gradients exerted by each particle, create explicit diffusion and velocity fields over the fluid that affects all the constituting particles in such a way that *anomalous diffusion* (in the form of *subdiffusion* and *superdiffusion*) and *non-ergodic behavior* is observed depending on the confinement of the particles.

Active particles are able to propel themselves in a fluid with low Reynolds number, *i.e.* in a fluid where viscosity dominates over inertial effects, so that mass of the particle can be neglected altogether. However, propulsion against viscosity and staying out of thermodynamic equilibrium requires energy. Biological microswimmers like bacteria use specialized flagella as the fuel of self-propulsion. Other swimmers, on the other hand, make use of phoresis in the form of chemotactic, electromagnetic or temperature gradients. For example, spherical Janus particles are artificial swimmers that are Pt-coated in one side. Inside an hydrogen peroxide solution, Pt-coated side of the spherical microparticle start to react with H_2O_2 which induces a local chemical gradient. Therefore, by heating the solution at desired locations with a laser beam to set off the reaction, self-propulsion may be achieved.

We put such microswimmers inside a square box with periodic boundary conditions so as to get rid of surface effects. Depending on the length of the square box, diffusion properties of the system is altered in a tunable fashion. When the

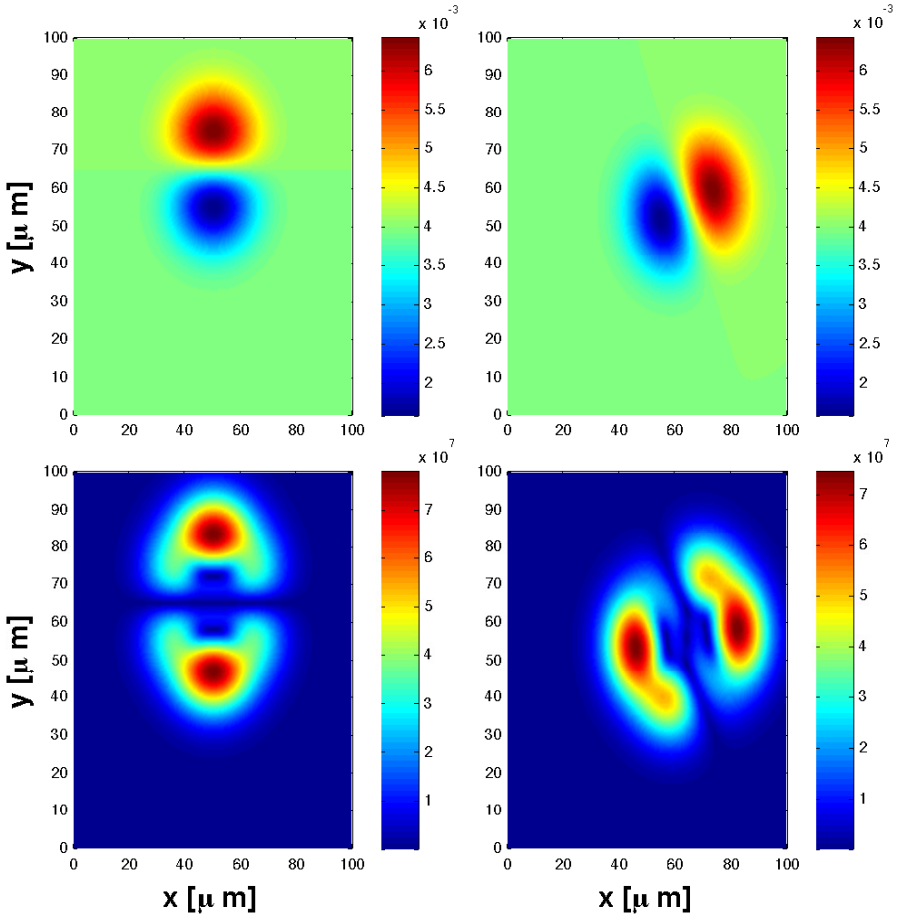

Figure 4.5: Diffusion (upper row) and noise-induced drift (lower row) fields for a particle oriented in the $\pi/2$ and $\pi/8$ directions. Both fields are oriented with the orientation of the particle. The nonuniform diffusion gradient describes attraction at long distances and repulsion at shorter distances.

confinement parameter c is large compared with the radius of the particles R, that is when the box is large and thereby particles are spaced away from each other, particles tend to affect each other in such a way that they show increased locomotion. As a result, particles are superdiffusive, with each particle having an MSD value that is proportional with t^{α} where $\alpha > 1$ as opposed to the ballistic regime of $\alpha = 1$. Moreover, the particles align each other to the same angle causing a transport phenomena.

When the confinement parameter c is small compared with R, on the other

hand, particles make each other slow down, thereby becoming subdiffusive, with MSD values proportional with t^{α} where $\alpha < 1$. Particle trajectories resemble that of continuous Brownian motion where particles wait a random time after each jump, in a sense time parameter itself is randomized as well as the step length. Continuous Brownian motion causes the mechanism of transient trapping in DNA gel electrophoresis and the subdiffusive motion of a colloidal tracer in an F-actin filament network [49, 50, 51].

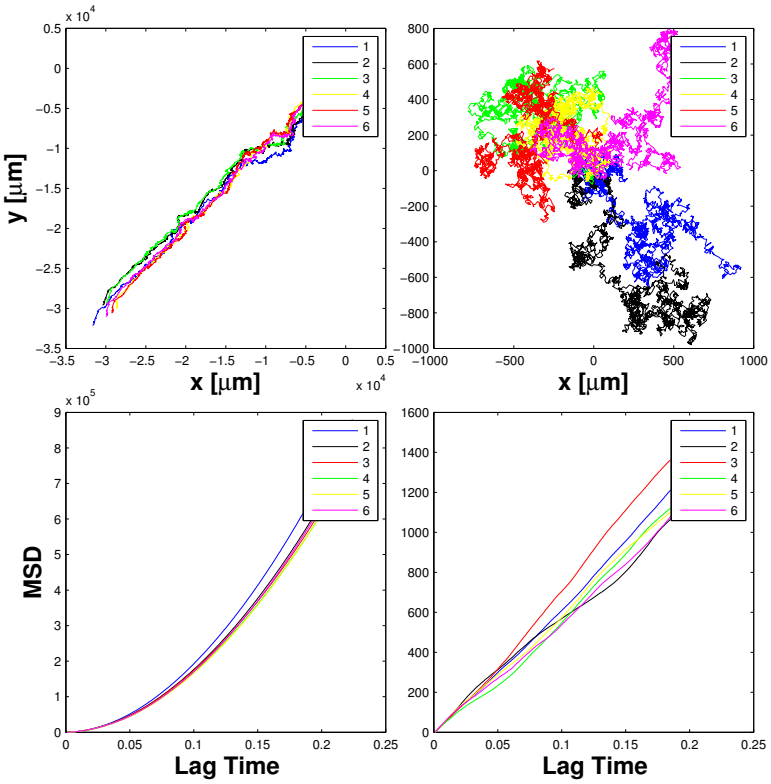

Figure 4.6: Trajectories (upper row) and MSD values (lower row) fields for 100 particles immersed in water. As is depicted in the first column, large confinement under periodic boundary conditions leads to superdiffusive behavior with phase-locking. In the second column, particles show Brownian motion characteristics as they are held in a smaller confinement space.

Model of DNA gel electrophoresis as a continuous time random walk process is mostly developed by Weiss in 1990's [52]. Within the model, electric field causes DNA molecules to pass through a porous gel, the rate of which depends on the size and charge of individual molecules. Small parts of DNA pass through

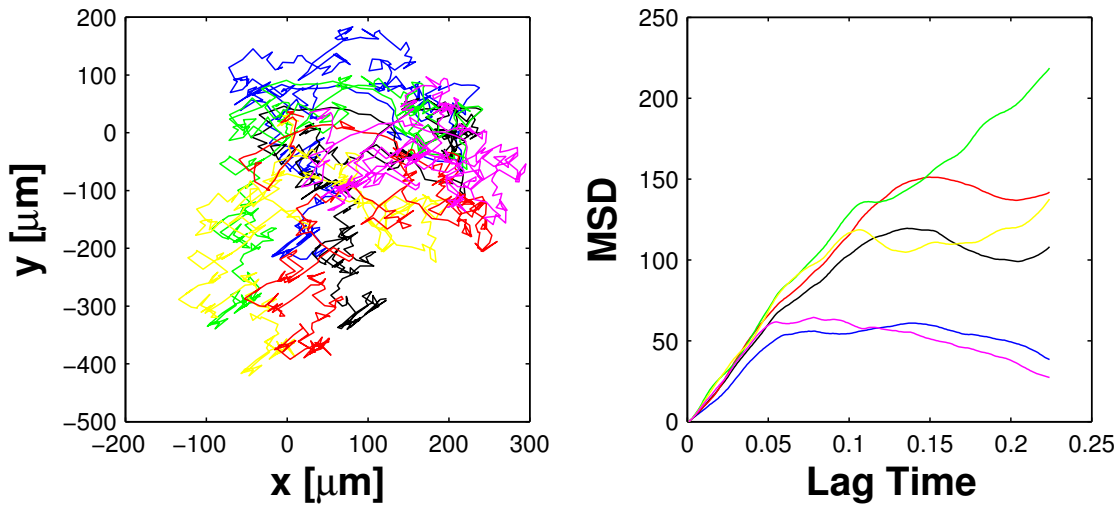

(a) Trajectory of the particles.

(b) MSD of the particles.

Figure 4.7: As the confinement becomes gets smaller and smaller, particles do continuous Brownian motion which has the characteristics of non-ergodicity and subdiffusion. For these graphs, confinement parameter $c = 1$, particle radius $R = 1\,\mu m$ and number of particles is $N = 6$.

the porous parts of gel whereas large molecules become trapped with very long waiting time between each displacement step which can be characterized as a random walk process with zero mean and finite variance as Weiss predicted. Incidentally, continous time random walk processes cause the emergence of non-ergodic behavior by breaking the conditions of ergodic hypothesis which states that all microstates of a system are equally probably to be occupied over a long period of time [53]. This is characterized by the fact that time averaged MSD and ensemble averaged MSD gives different results in stark contrast to an ergodic system. In our model, non-ergodic subdiffusion in the form of continuous time random walk occurs as a result of inhomegenous nature of the environment caused by confinement of the particles with varying diffusivities in a rather small volume.

4.3 Particle Sorting with Noise-Induced Drift

Multiplicative noise arises in the study of stochastic differential equations to comply with mathematical models that involve noise terms which depend on the state of the system. There is an intrinsic ambiguity with such systems with multiplicative noise, rooted in the modeling of randomness. Here, we make use of this mathematical ambiguity to design a microparticle sorter that separates micoparticles depending on their radius by inducing a diffusion gradient by means of confinement of Brownian particles immersed in a fluid in between two walls and thereby driving the particles with a noise-induced drift which arises from the induced diffusion gradient.

A general stochastic differential equation with multiplicative noise in functional form is described by:

$$dy_t = \underbrace{f(y_t)dt}_{\text{Drift term}} + \underbrace{\sigma g(y_t)dW_t}_{\text{Diffusion term}} \tag{4.16}$$

where σ is the noise intensity and dW_t describes the time derivative of the white noise with zero mean, finite variance and delta correlation, for which drift term constitutes the deterministic part of the stochastic differential equation, whereas diffusion term models that of a random process [20]. Unlike the case with additive noise, when multiplicative noise term that describes the dependance of the noise on the state of the system is involved, evaluation of the integral with the white noise term in the solution of the SDE requires careful attention on the grounds that white noise is not bounded, therefore it cannot be approximated with Riemann-Stieltjes sums of ordinary differential calculus. The second term on the right hand side of equation 4.16 can be evaluated in general form of $\int_0^\tau g(y_t) \circ_\alpha dW_t \equiv \lim_{N\to+\infty} \sum_{n=0}^{N-1} g(y_{t_n}) \Delta W_{t_n}$ with $t_n = \frac{n+\alpha}{N}\tau$ and $\alpha \epsilon (0,1)$ where different values of α correspond to different stochastic calculus conventions. When the system is coupled to a heat bath, as is the case for a Brownian particle, maximum value of $\alpha = 1$ is chosen so as to reproduce the thermal equilibrium condition [19].

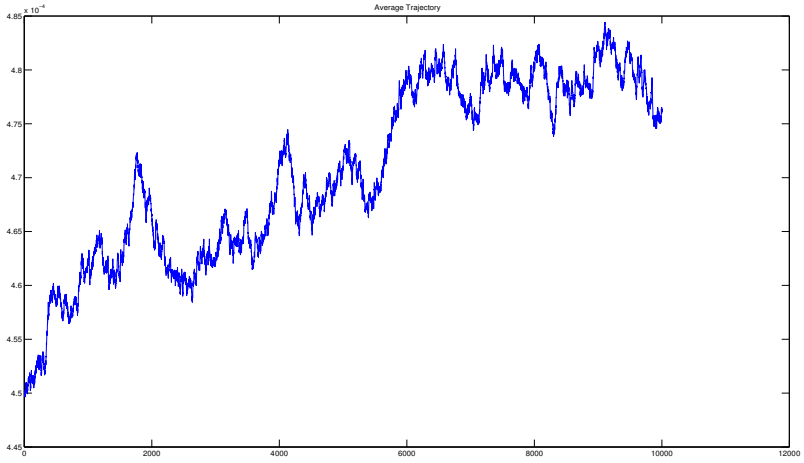

Figure 4.8: Average trajectory of a 100 realizations.

In order to make use of this maximal noise-induced drift, a diffusion gradient is induced by confining a Brownian particle immersed in a fluid between two walls where one of the walls is convex so as to make the noise-induced drift term linear. For such a configuration, diffusion is given by the equation:

$$D(h(x),z) = \frac{k_B T}{\gamma} \frac{1}{\lambda(\frac{R}{z}) + \lambda(\frac{R}{h(x)-z}) - 1)} \tag{4.17}$$

where the function λ is described with $\lambda = [1 - \frac{9}{16}\frac{R}{z} + \frac{1}{8}(\frac{R}{z})^3 - \frac{45}{256}(\frac{R}{z})^4 - \frac{1}{16}(\frac{R}{z})^5]^{-1}$ in which z is the direction perpendicular to the two walls and h is the height profile of the upper wall which is given by $h(x) = h_0 x^2 + c$ where x is the direction parallel to the walls. With this state-dependent diffusion coefficient, the discretized Langevin equation turns into:

$$x(j+1) = x(j) + \underbrace{\sqrt{2D(x)dt}dW}_{\text{Diffusion Term}} + \underbrace{\alpha \frac{dD(x)}{dx} dt}_{\text{Spurious Drift Term}} \tag{4.18}$$

for which, for a 1 μm radius particle with $\xi = 0.99 \times 10^{-3}$ $\frac{kg}{ms}$ viscosity and an initial height of $z = 1.1 \times 10^{-3}$ μm, diffusion coefficient is significantly reduced from that of bulk value and a noise-induced drift term proportional with the

diffusion gradient is induced.

Under thermal equilibrium, the choice of anti-Itô stochastic calculus convention induces a noise-induced drift term that drives the probability distribution of the particle displacement towards the more positive side in the positive axis and towards the more negative side when the particle is in the negative axis. Figure 4.9a shows that, for a particle with 1 μm radius, probability distribution of possible displacements of 30000 non-interacting particles changes accordingly with the induced noise-induced drift by the diffusion gradient. To quantify this change, centers of masses of each corresponding histogram bin is calculated which implies that histogram corresponding to the probability distribution of these particle displacements shifts linearly under the action of noise-induced drift.

Since for a particle with different radius, diffusion coefficient changes which in turn changes the noise-induced drift term, thereby producing a different shift in the probability distribution of the corresponding particle displacements, it is in principle possible to use this effect as a microparticle sorter via funnels.

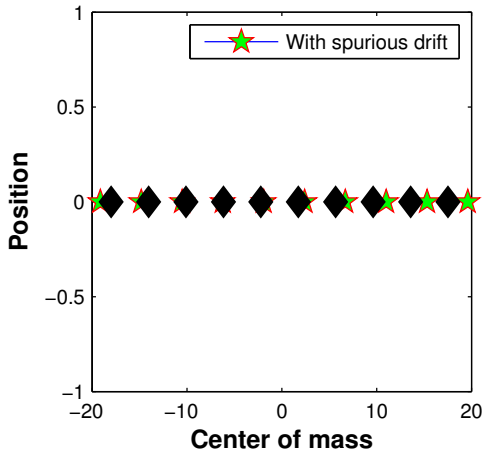

(a) Shift in the center of masses for the histogram bins.

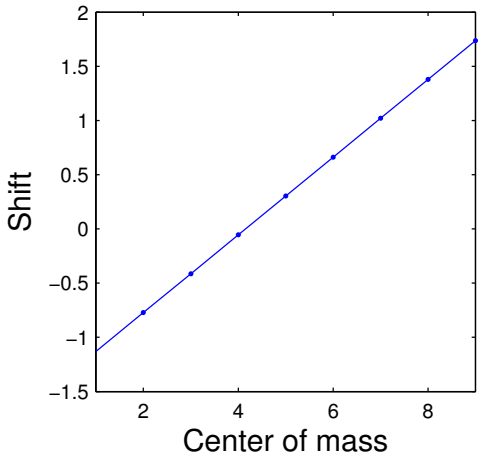

(b) Linear increase of the shift in center of masses of histogram bins.

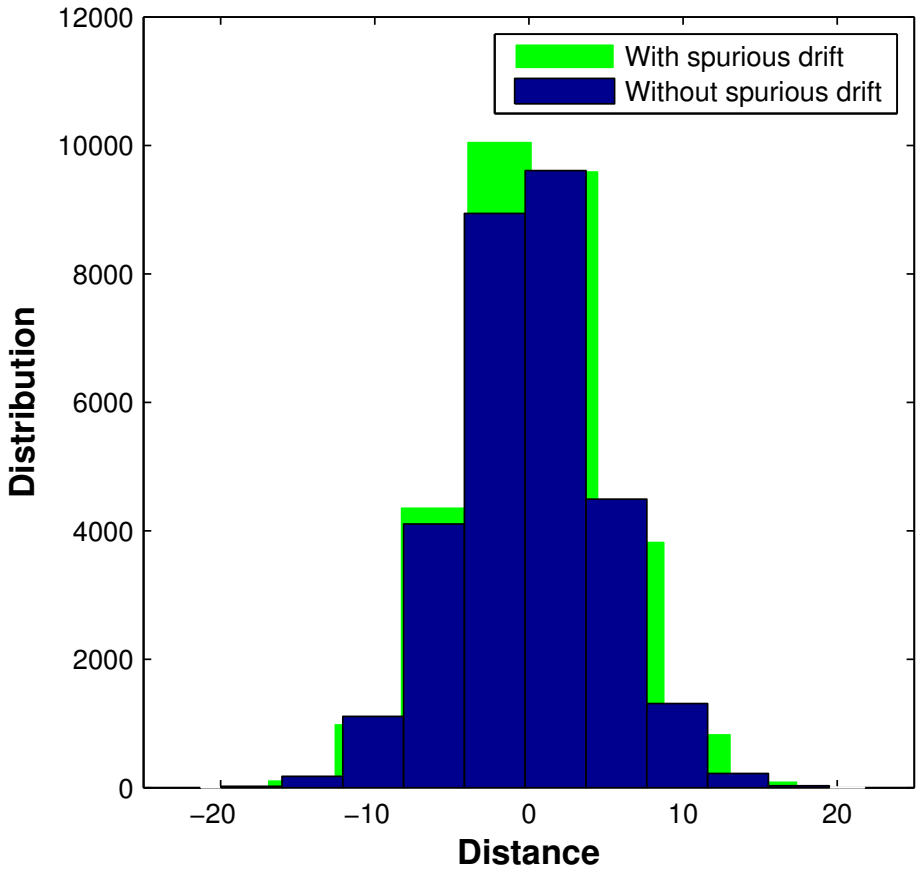

(c) Histogram depicting the distribution of particle displacements for the cases with and without noise-induced drift.

Figure 4.9: Shift in the probability distribution due to the noise-induced drift.

Chapter 5

Conclusion and Prospects

Even though randomness has always been a fascination for human beings in the conquest of unknowable, mathematical formulation of random phenoma had intensified heavily relatively recently with the advent of quantum mechanics and the developments in finance. Combining it with nonlinear systems, which describes most of the phenomena in nature, is a crucial step towards a concise and complete mathematical formalism of randomness which can help us predicting future outcome of events better as well as making more accurate predictions about long past retrospectively. In this thesis, we have paved the way for a better understanding of randomness coupled into nonlinear systems.

We reported that noise changes the nonlinear dynamics intrinsic to a system dynamically by inducing a finite drift over the phase space of the system. We studied the effects and possible applications of this noise-induced drift in several systems from ecology and soft matter physics.

We showed that, for an ecological system with two species competing for the same resource, the evolution of populations in time depends upon the nature of the noise. The population with a short feedback delay time (*i.e.*, the time it takes for a species to reach the adult state from the egg state) compared with the other species wins the competition by dominating over the other species as a result of stochastic calculus convention it obeys exerting a larger drift on it.

The work with ecological systems led us to consider the effects of the noise-induced drift in nonequilibrium systems from statistical and soft matter physics. We studied the collective behavior of microswimmer interacting via nonuniform diffusion gradients and showed that there is tunable anomalous diffusion depending on the confinement length of swimmers altering the noisy behavior. Diffusion characteristics of micro and nanoparticles under nonequilibrium conditions are important in microrheology, drug delivery and cargo transport.

We proposed a method to make use of this effect in a useful application by proposing a microparticle sorter based on the noise-induced drift resulting from the confinement of particles in certain geometries which lead to nonuniform gradients of diffusion. By this way, we showed numerically that it is possible to sort spherical microparticles with governing the underlying noise carefully without using any real force arising from a potential energy gradient.

Finally, we developed an approximation method that converts stochastic differential delay equations to stochastic differential equations which is much easier to study, because the theory and tools are far more developed comparatively.

Gaining new insights on the ways noise affects the nonlinear dynamics will pave the way for future researchers on developing technology by manipulating the noise in an applicable way especially at the micro- and nano-scale. Therefore, understanding and controlling the underlying noise is a very important step in human-made technology that mimicks nature. In particular techniques based on noise manipulation can be especially useful in applications where noise can provide the energy such as pattern formation at the nanoscale, drug delivery, cargo transport in microfluidic channels, nanophotonics and Brownian ratchets.

Bibliography

[1] J. Burnet, *Greek Philosophy: Thales to Plato*, vol. 1. Macmillan, 1914.

[2] D. W. Graham, *Aristotle Physics*, vol. 3. Oxford University Press, 1999.

[3] A. Einstein, "Über die von der molekularkinetischen Theorie der Wärme geforderte Bewegung von in ruhenden Flüssigkeiten suspendierten Teilchen," *Annalen der Physik*, vol. 322, pp. 549–560, 1905.

[4] K. Itô, "Stochastic integral," *Proc. Japan Acad. A*, vol. 20, pp. 519–524, 1994.

[5] R. Stratonovich, "A new representation for stochastic integrals and stochastic differential equations," *SIAM J. Control*, vol. 4, pp. 362–371, 1966.

[6] S. Hottovy, G. Volpe, and J. Wehr, "Noise-induced drift in stochastic differential equations with arbitrary friction and diffusion in the smoluchowski-kramers limit," *Journal of Statistical Physics*, vol. 146, no. 4, pp. 762–773, 2012.

[7] P. Lançon, G. Batrouni, L. Lobry, and N. Ostrowsky, "Drift without flux: Brownian walker with a space-dependent diffusion coefficient," *EPL (Europhysics Letters)*, vol. 54, no. 1, p. 28, 2001.

[8] J. Smythe, F. Moss, and P. V. McClintock, "Observation of a noise-induced phase transition with an analog simulator," *Physical review letters*, vol. 51, no. 12, p. 1062, 1983.

[9] G. Volpe, L. Helden, T. Brettschneider, J. Wehr, and C. Bechinger, "Influence of noise on force measurements," *Phys. Rev. Lett.*, vol. 104, p. 170602, Apr 2010.

[10] T. Brettschneider, G. Volpe, L. Helden, J. Wehr, and C. Bechinger, "Force measurement in the presence of brownian noise: Equilibrium-distribution method versus drift method," *Phys. Rev. E*, vol. 83, p. 041113, Apr 2011.

[11] N. Van Kampen, "Itô versus stratonovich," *Journal of Statistical Physics*, vol. 24, no. 1, pp. 175–187, 1981.

[12] A. W. C. Lau and T. C. Lubensky, "State-dependent diffusion: Thermodynamic consistency and its path integral formulation," *Phys. Rev. E*, vol. 76, p. 011123, Jul 2007.

[13] Y. L. Klimontovich, "Ito, stratonovich and kinetic forms of stochastic equations," *Physica A: Statistical Mechanics and its Applications*, vol. 163, no. 2, pp. 515–532, 1990.

[14] R. Kupferman, G. Pavliotis, and A. Stuart, "Itô versus stratonovich white-noise limits for systems with inertia and colored multiplicative noise," *Physical Review E*, vol. 70, no. 3, p. 036120, 2004.

[15] G. Pesce, A. McDaniel, S. Hottovy, J. Wehr, and G. Volpe, "Stratonovich-to-Itô transition in noisy systems with multiplicative feedback," *Nature Communications*, 2013.

[16] L. Gammaitoni, P. Hänggi, P. Jung, and F. Marchesoni, "Stochastic resonance," *Reviews of modern physics*, vol. 70, no. 1, p. 223, 1998.

[17] K. Wiesenfeld, F. Moss, *et al.*, "Stochastic resonance and the benefits of noise: from ice ages to crayfish and squids," *Nature*, vol. 373, no. 6509, pp. 33–36, 1995.

[18] J. K. Douglass, L. Wilkens, E. Pantazelou, and F. Moss, "Noise enhancement of information transfer in crayfish mechanoreceptors by stochastic resonance," *Nature*, vol. 365, no. 6444, pp. 337–340, 1993.

[19] P. E. Kloeden and E. Platen, *Numerical solution of stochastic differential equations*, vol. 23. Springer, 1992.

[20] B. Oksendal, *Stochastic Differential Equations: An Introduction with Applications*. Springer, 5 ed., 1998.

[21] N. Wiener, *Time Series*. MIT Press, 9 ed., 1964.

[22] A. Khintchine, "Korrelationstheorie der stationären stochastischen Prozesse," *Mathematische Annalen*, vol. 109, pp. 604–615, 1934.

[23] H. Risken, *The Fokker-Planck Equation*. Springer-Verlag, 2 ed., 1989.

[24] I. Karatzas and S. Shreve, *Brownian Motion and Stochastic Calculus*. Springer, 2 ed., 1998.

[25] N. G. van Kampen, *Stochastic Processes in Physics and Chemistry*. North Holland, 3 ed., 2007.

[26] E. Wong and M. Zakai, "On the convergence of ordinary integrals to stochastic integrals," *Ann. Math. Stat.*, vol. 36, no. 5, pp. 1560–1564, 1965.

[27] H. Berg, *E. Coli in Motion*. Springer-Verlag, 3 ed., 2004.

[28] E. Lauga and R. E. Goldstein, "Dance of the microswimmers," *Physics Today*, vol. 65, no. 9, pp. 30–35, 2012.

[29] A. Walther and A. H. E. Müler, "Janus particles: Synthesis, self-assembly, physical properties, and applications," *Chemical Reviews*, vol. 113, no. 7, pp. 5194–5261, 2013.

[30] G. Volpe and G. Volpe, "Simulation of a brownian particle in an optical trap," *American Journal of Physics*, vol. 81, no. 3, pp. 224–230, 2013.

[31] G. E. Uhlenbeck and L. S. Ornstein, "On the theory of brownian motion," *Phys. Rev.*, vol. 36, pp. 832–841, 1930.

[32] D. T. Gillespie, "Exact numerical simulation of the ornstein-uhlenbeck process and its integral," *Phys. Rev. E*, vol. 54, pp. 2084–2091, 1996.

[33] J. L. Doob, "The brownian movement and stochastic equations," *Annals of Mathematics*, vol. 43, pp. 351–369, 1942.

[34] E. Wong and M. Zakai, "On the convergence of ordinary integrals to stochastic integrals," *The Annals of Mathematical Statistics*, vol. 36, no. 5, pp. 1560–1564, 1965.

[35] D. Frenkel and B. Smit, *Understanding molecular simulation: from algorithms to applications*, vol. 1. Academic press, 2001.

[36] V. Volterra, "Variazioni e fluttuazioni del numero dindividui in specie animali conviventi," *Mem. Acad. Lincei Roma*, vol. 2, pp. 31–113, 1926.

[37] L. Nie and D. Mei, "Effects of time delay on symmetric two-species competition subject to noise," *Phys. Rev. E*, vol. 77, p. 031107, 2008.

[38] R. Rudnicki and K. Pichor, "Influence of stochastic perturbation on prey-predator systems," *Mathematical Biosciences*, vol. 206, pp. 108–119, 2007.

[39] B. Spagnolo, S. Spezia, L. Curcio, N. Pizzolato, A. Fiasconaro, D. Valenti, P. Lo Bue, E. Peri, and S. Colazza, "Noise effects in two different biological systems," *The European Physical Journal B*, vol. 69, no. 1, pp. 133–146, 2009.

[40] B. Spagnolo and A. La Barbera, "Role of the noise on the transient dynamics of an ecosystem of interacting species," *Physica A: Statistical Mechanics and its Applications*, vol. 315, no. 1, pp. 114–124, 2002.

[41] A. Dobrinevski and E. Frey, "Extinction in neutrally stable stochastic lotka-volterra models," *Phys. Rev. E*, vol. 85, p. 051903, 2012.

[42] P. Mandal and M. Banerjee, "Multiplicative-noise can suppress chaotic oscillation in lotka-volterra type competitive model," *Mathematical Modelling of Natural Phenomena*, vol. 7, pp. 23–46, 1 2012.

[43] C. R. Ruetz, J. C. Trexler, F. Jordan, W. F. Loftus, and S. A. Perry, "Population dynamics of wetland fishes: Spatio-temporal patterns synchronized by hydrological disturbance?," *Journal of Animal Ecology*, vol. 74, no. 2, pp. pp. 322–332, 2005.

[44] D. Valenti, A. Fiasconaro, and B. Spagnolo, "Stochastic resonance and noise delayed extinction in a model of two competing species," *Physica A: Statistical Mechanics and its Applications*, vol. 331, no. 34, pp. 477 – 486, 2004.

[45] J. D. Murray, *Mathematical Biology*. Springer, 2 ed., 2002.

[46] S. H. Strogatz, *Nonlinear Dynamics and Chaos*. Westview Press, 1 ed., 2001.

[47] B. Caetano Troca Cabella, A. Souto Martinez, and F. Ribeiro, "Full analytical solution and complete phase diagram analysis of the Verhulst-like two-species population dynamics model," *ArXiv e-prints*, 2010.

[48] A. McDaniel, O. Duman, G. Volpe, and J. Wehr, "An SDE approximation for stochastic differential delay equations with colored state-dependent noise," *ArXiv e-prints*, 2014.

[49] I. Wong, M. Gardel, D. Reichman, E. R. Weeks, M. Valentine, A. Bausch, and D. Weitz, "Anomalous diffusion probes microstructure dynamics of entangled f-actin networks," *Phys. Rev. Lett.*, vol. 92, no. 17, p. 178101, 2004.

[50] B. Wang, S. M. Anthony, S. C. Bae, and S. Granick, "Anomalous yet brownian," *Proceedings of the National Academy of Sciences*, vol. 106, no. 36, pp. 15160–15164, 2009.

[51] J. F. Robyt and B. J. White, *Biochemical Techniques Theory and Practice*. Waveland Press, 2 ed., 1990.

[52] G. H. Weiss, M. Garner, E. Yarmola, P. Boček, and A. Chrambach, "A comparison of resolution of dna fragments between agarose gel and capillary zone electrophoresis in agarose solutions," *Electrophoresis*, vol. 16, no. 1, pp. 1345–1353, 1995.

[53] L. Boltzmann, *Vorlesungen über Gastheorie*, vol. 1. Verlag von Johann Ambrosius Barth, 1896.

Appendix A

Code

A.1 Free Diffusion

Matlab code for calculating the evolution of a Brownian particle under free diffusion conditions:

```
clear all; close all; clc;

N = 1e+3;
dt = 1e-2;
sqrtDt = sqrt(dt);
t = dt*(1:N);

x = zeros(1,N+1);
w = randn(1,N+1);

for j = 1:N
    x(j+1) = x(j) + sqrtDt*randn();
end
```

A.2 Colored Noise

Matlab code for calculating colored noise with Ornstein-Uhlenbeck process with exponential correlation:

```
function ceta = cnoise(tau,dt,N)
% Generation of correlated noise
%
% tau = correlation time [s]
% dt = timestep [s]
% N = number of samples
%
% ceta = normalized colored noise with correaltion time tau

eta = randn(1,N);
ceta = zeros(1,N);
rho = exp(-dt/tau);
for i = 1:1:N-1
    ceta(i+1) = rho*ceta(i) + sqrt(1-rho^2)*eta(i+1);
end

ceta = ceta/sqrt(2*tau);
```

A.3 Monte Carlo Simulatoin of Collective Behavior of Microswimmers

A.3.1 Diffusion Field Calculation

Matlab function to calculate the diffusion coefficient at each configuration of positions of the particles:

```
function [D,sx,sy] ...
= sdiffield(x1,y1,x2,y2,phi,varargin)
```

```
% SDIFFIELD   Calculates the diffusion and the spurious drift induced by
% the diffusion field of a mesoscopic particle

sx = 15e-6*cos(phi);
sy = 15e-6*sin(phi);
rx = x2-x1-sx;
ry = y2-y1-sy;
r = sqrt(rx^2+ry^2);
Dc = 5e-15;

A = 1e-14; % normalization constant
w = 1e-5; % width
k = (A/(w*sqrt(2*pi)));

D =  Dc + gaussianfnc(r,k,w)*(rx*cos(phi) + ry*sin(phi)); % diffusion [m^2/s]
sx = -rx*gaussianfnc(r,k,w)/w^2*(cos(phi)-(2*rx/w^2)*(rx*cos(phi)+ry*sin(phi)))
sy = -ry*gaussianfnc(r,k,w)/w^2*(sin(phi)-(2*ry/w^2)*(rx*cos(phi)+ry*sin(phi)))
```

A.3.2 Gaussian Function

Matlab function to generate a Gaussian function which is used in the calculation of the diffusion coefficient:

```
function [ g ] = gaussianfnc( r,k,w )
%GAUSSIANFNC Gives a 2D Gaussian function
%   INPUTS:
%   r: point in 2D
%   k: constant
%   w: standard deviation

g = k*exp(-r^2/(2*w^2));

end
```

A.3.3 Distance Calculation

Matlab function to calculate the distance between individual particles:

```
function [ d ] = distcalc( xn,yn,x,y )
%DISTCALC Calculates distance between particle n and the other particles
%   INPUTS:
%   xn          source particle position in the x direction [m]
%   yn          source particle position in the y direction [m]
%   x           target particle positions in the x direction [m]
%   y           target particle positions in the y direction [m]
%
%   OUTPUT:
%   d           distance between the particles [m]
%

% Get the displacement
dx = abs(x - xn);
dy = abs(y - yn);
d = sqrt(dx^2 + dy^2);


end
```

A.3.4 Periodic Boundary Conditions

Matlab function to generate periodic boundary conditions inside a square box for the particles at their respective positions:

```
function [ x,y ] = PBC( x,y,L )
%PBC Applies periodic boundary conditions in 2D
%   INPUTS:
%   x       coordinate in x direction [m]
%   y       coordinate in y direction [m]
%   L       box size [m]
%
```

```
%   OUTPUTS:
%   x       coordinate in x direction [m]
%   y       coordinate in y direction [m]
%


if (x > L)
    x = x - L;
elseif (x < 0)
    x = x + L;
end

if (y > L)
    y = y - L;
elseif (y < 0)
    y = y + L;
end

end
```

A.3.5 Initial Conditions

Matlab function for calculating the initial conditions inside a square box with periodic boundary conditions:

```
function [ px,py,L ] = initPositions( M,R,c )
%INITPOSITIONS Initialize the positions of the particles for a square
% lattice
%   INPUTS:
%   M       number of particles
%   R       radius of the particle [m]
%   c       density constant for the particles [m]
%
%   OUTPUTS:
%   px      initial position in x of all the particles [m] -- Mx1 matrix
%   py      initial position in y of all the particles [m] -- Mx1 matrix
%   L       box size [m]
```

```
    %

    % Preallocation
    p = zeros(M,2);

    % Box size calculation
    L = M*2*R + c;

    % Lowest number of squares at the number of particles
    nSquare = 2;

    while (nSquare^2 < M)
       nSquare = nSquare + 1;
    end

    index = [0,0]';

    % Assign particle positions
    for m = 1:M

        p(m,:) = (index+[0.5,0.5]')*(L/nSquare);

        index(1) = index(1) + 1;
        if (index(1) == nSquare)
            index(1) = 0;
            index(2) = index(2) + 1;
        end

    end

px = p(:,1);
py = p(:,2);

end
```

A.3.6 Monte Carlo Simulation

Matlab script for calculating particle displacements with a hard sphere Monte Carlo simulation:

```
%% Multiple hard sphere Brownian particles
% under the effect of diffusion gradient

%% Initialization of the workspace
close all; clear all; clc;
tic


%% Parameters

% Set simulation parameters
N = 1e+5; % number of steps
dt = 1e-3; % step size [s]
sqrtDt = sqrt(dt); % square root of time step
printFreq = 1000; % printing frequency
sampleFreq = 2; % sampling frequency
sampleCounter = 1; % sampling counter
t = dt*[0:sampleFreq:N]; % time [s]

% Set the properties of the spherical particle
R = 1e-6; % radius [m]
M = 20; % number of particles
v = 5e-11; % velocity [m/s]

% Set the properties of the medium
T = 300; % temperature [K] --room temp. = 300 K
eta = 0.001; % viscosity [Ns/m^2] --water = 0.001
kB = 1.38e-23; % Boltzmann constant [J/K]
c = 100e-6; % density constant for the particles [m]
rc = 20e-6; % cutoff distance for calculation of diffusion [m]
Dr = kB*T/(8*pi*eta*R^3); % rotational diffusion coefficient [rad^2/s]
```

```
%% Simulation

%
% Preallocation and initialization
pa = zeros(M,N+1); % particle orientation [rad]
pa(:,1) = 2*pi*randn();
px = zeros(M,N/sampleFreq); % particle position in x [m]
py = zeros(M,N/sampleFreq); % particle position in y [m]
% [x,y,L] = initPositions(M,R,c); % initial positions [m]
L = M*2*R + c;
x(:,1) = L*randn(1,M);
y(:,1) = L*randn(1,M);
D = zeros(M,M); % diffusion matrix [m^2/s]
sx = zeros(M,M); % spurious drift matrix in x [m/s]
sy = zeros(M,M); % spurious drift matrix in y [m/s]
Di1 = zeros(M,M);
sxi1 = zeros(M,M);
syi1 = zeros(M,M);
Di2 = zeros(M,M);
sxi2 = zeros(M,M);
syi2 = zeros(M,M);
Di3 = zeros(M,M);
sxi3 = zeros(M,M);
syi3 = zeros(M,M);
Di4 = zeros(M,M);
sxi4 = zeros(M,M);
syi4 = zeros(M,M);
%

%
% Create the image list
for m = 1:M
    pxi(m,1) = x(m,1) + L; % first image in x
    pxi(m,2) = x(m,1) - L; % second image in x
    pyi(m,1) = y(m,1) + L; % first image in y
    pyi(m,2) = y(m,1) - L; % second image in y
end
%

%
```

```
% Calculate initial diffusion field D(m,j) where mth particle affects
% the jth particle
for m = 1:M
    for j = 1:M

        d1 = distcalc(x(m,1),y(m,1),x(j,1),y(j,1));
        if (d1 < rc)
            [D(m,j),sx(m,j),sy(m,j)] = ...
                sdiffield(x(m,1),y(m,1), ...
                x(j,1),y(j,1),pa(m,1));
        else
            D(m,j) = 0;
            sx(m,j) = 0;
            sy(m,j) = 0;
        end

        di1 = distcalc(x(m,1),y(m,1),pxi(j,1),pyi(j,1));
        if (di1 < rc)
            [Di1(m,j),sxi1(m,j),syi1(m,j)] = ...
                sdiffield(x(m,1),y(m,1), ...
                pxi(j,1),pyi(j,1),pa(m,1));
        else
            Di1(m,j) = 0;
            sxi1(m,j) = 0;
            syi1(m,j) = 0;
        end

        di2 = distcalc(x(m,1),y(m,1),pxi(j,1),pyi(j,2));
        if (di2 < rc)
            [Di2(m,j),sxi2(m,j),syi2(m,j)] = ...
                sdiffield(x(m,1),y(m,1), ...
                pxi(j,1),pyi(j,2),pa(m,1));
        else
            Di2(m,j) = 0;
            sxi2(m,j) = 0;
            syi2(m,j) = 0;
        end

        di3 = distcalc(x(m,1),y(m,1),pxi(j,2),pyi(j,1));
        if (di3 < rc)
```

```
            [Di3(m,j),sxi3(m,j),syi3(m,j)] = ...
                sdiffield(x(m,1),y(m,1), ...
                pxi(j,2),pyi(j,1),pa(m,1));
        else
            Di3(m,j) = 0;
            sxi3(m,j) = 0;
            syi3(m,j) = 0;
        end

        di4 = distcalc(x(m,1),y(m,1),pxi(j,2),pyi(j,2));
        if (di4 < rc)
            [Di4(m,j),sxi4(m,j),syi4(m,j)] = ...
                sdiffield(x(m,1),y(m,1), ...
                pxi(j,2),pyi(j,2),pa(m,1));
        else
            Di4(m,j) = 0;
            sxi4(m,j) = 0;
            syi4(m,j) = 0;
        end

    end
end
%

%
% Evaluation through Brownian dynamics
for n = 1:N  % time step index

    for m = 1:M % particle number index

        % Suggest a move based on Langevin equations
        % Rotational Langevin equation
        pa(m,n+1) = pa(m,n) + sqrt(2*Dr)*sqrtDt*randn();

        % Langevin equation in x
        xTrial = ...
            + sqrt(2*(sum(D(:,m))+sum(Di1(:,m))+sum(Di2(:,m)) ...
            + sum(Di3(:,m))+sum(Di4(:,m))))*sqrtDt*randn() ...
            + (sum(sx(:,m))+sum(sxi1(:,m))+sum(sxi2(:,m)) ...
            + sum(sxi3(:,m))+sum(sxi4(:,m)))*dt ...
```

```
    + v*cos(pa(m,n+1));

% Langevin equation in y
yTrial = ...
    + sqrt(2*(sum(D(:,m))+sum(Di1(:,m))+sum(Di2(:,m)) ...
    + sum(Di3(:,m))+sum(Di4(:,m))))*sqrtDt*randn() ...
    + (sum(sy(:,m))+sum(syi1(:,m))+sum(syi2(:,m)) ...
    + sum(syi3(:,m))+sum(syi4(:,m)))*dt ...
    + v*sin(pa(m,n+1));


% Check for collisions between the particles
for j = 1:M % particle collision start

    % Compare only to particle
    % that are not the one being moved
    if (j ~= m)
        % Calculate the distance
        % between particle m and the other particles
        dst = distcalc(x(m,1)+xTrial,y(m,1)+yTrial, ...
            x(j,1),y(j,1));
        dst1 = distcalc(x(m,1)+xTrial,y(m,1)+yTrial, ...
            pxi(m,1),pyi(m,1));
        dst2 = distcalc(x(m,1)+xTrial,y(m,1)+yTrial, ...
            pxi(m,1),pyi(m,2));
        dst3 = distcalc(x(m,1)+xTrial,y(m,1)+yTrial, ...
            pxi(m,2),pyi(m,1));
        dst4 = distcalc(x(m,1)+xTrial,y(m,1)+yTrial, ...
            pxi(m,2),pyi(m,2));

        % Check if there is a collision
        check = true;
        if ( dst<2*R || dst1<2*R || dst2<2*R || dst3<2*R || dst4<2*R )
            check = false;
        end

        % Accept the move if there's no collision
        if (check == true)
           x(m,1) = x(m,1) + xTrial;
           y(m,1) = y(m,1) + yTrial;
```

```
            end
        end

    end % particle collision end

    % Check if the particles are in the box
    % with periodic boundary conditions
    [x(m,1),y(m,1)] = PBC(x(m,1),y(m,1),L);

end % particle number end

% Do sampling
if (mod(n,sampleFreq) == 0)
    px(sampleCounter) = x(m,1);
    py(sampleCounter) = y(m,1);
    sampleCounter = sampleCounter + 1;
end

%     % Print the step
%     if (mod(n,printFreq)==0)
%         n
%         plot(x(:,1),y(:,1),'o')
%         drawnow()
%     end

for m = 1:M
    % Create the image list
    pxi(m,1) = x(m,1) + L; % first image in x
    pxi(m,2) = x(m,1) - L; % second image in x
    pyi(m,1) = y(m,1) + L; % first image in y
    pyi(m,2) = y(m,1) - L; % second image in y
end


% Calculate the diffusion field D(m,j)
% where mth particle affects
% the jth particle
for m = 1:M
    for j = 1:M
```

```
d1 = distcalc(x(m,1),y(m,1),x(j,1),y(j,1));
if (d1 < rc)
    [D(m,j),sx(m,j),sy(m,j)] = ...
        sdiffield(x(m,1),y(m,1), ...
        x(j,1),y(j,1),pa(m,n+1));
else
    D(m,j) = 0;
    sx(m,j) = 0;
    sy(m,j) = 0;
end

di1 = distcalc(x(m,1),y(m,1),pxi(j,1),pyi(j,1));
if (di1 < rc)
    [Di1(m,j),sxi1(m,j),syi1(m,j)] = ...
        sdiffield(x(m,1),y(m,1), ...
        pxi(j,1),pyi(j,1),pa(m,n+1));
else
    Di1(m,j) = 0;
    sxi1(m,j) = 0;
    syi1(m,j) = 0;
end

di2 = distcalc(x(m,1),y(m,1),pxi(j,1),pyi(j,2));
if (di2 < rc)
    [Di2(m,j),sxi2(m,j),syi2(m,j)] = ...
        sdiffield(x(m,1),y(m,1), ...
        pxi(j,1),pyi(j,2),pa(m,n+1));
else
    Di2(m,j) = 0;
    sxi2(m,j) = 0;
    syi2(m,j) = 0;
end

di3 = distcalc(x(m,1),y(m,1),pxi(j,2),pyi(j,1));
if (di3 < rc)
    [Di3(m,j),sxi3(m,j),syi3(m,j)] = ...
        sdiffield(x(m,1),y(m,1), ...
        pxi(j,2),pyi(j,1),pa(m,n+1));
else
    Di3(m,j) = 0;
```

```
                sxi3(m,j) = 0;
                syi3(m,j) = 0;
            end

            di4 = distcalc(x(m,1),y(m,1),pxi(j,2),pyi(j,2));
            if (di4 < rc)
                [Di4(m,j),sxi4(m,j),syi4(m,j)] = ...
                    sdiffield(x(m,1),y(m,1), ...
                    pxi(j,2),pyi(j,2),pa(m,n+1));
            else
                Di4(m,j) = 0;
                sxi4(m,j) = 0;
                syi4(m,j) = 0;
            end


        end
    end

end % time step end
%

%
% Unfolding the trajectory
for m = 1:M
    px(m,:) = (L/(2*pi))*unwrap(px(m,:)*2*pi/L);
    py(m,:) = (L/(2*pi))*unwrap(py(m,:)*2*pi/L);
end
%

%
% Calculation of MSD

% Time averaged MSD
r = sqrt(px.^2 + py.^2);
msd = zeros(M,ceil(sqrt(length(r))));
for m = 1:M
    for n = 0:1:sqrt(length(r))
        msd(m,n+1) = mean((r(m,n+1:end)-r(m,1:end-n)).^2);
    end
```

```
end
u = dt*[1:1:length(msd)];
%

%% Plot

N = N/sampleFreq;

%%

%
% Plot of trajectories in a common figure
figure;
hold on
plot(px(1,:)*1e+6,py(1,:)*1e+6)
plot(px(2,:)*1e+6,py(2,:)*1e+6,'Color','k')
plot(px(3,:)*1e+6,py(3,:)*1e+6,'Color','g')
plot(px(4,:)*1e+6,py(4,:)*1e+6,'Color','y')
plot(px(5,:)*1e+6,py(5,:)*1e+6,'Color','r')
plot(px(6,:)*1e+6,py(6,:)*1e+6,'Color','m')
hold off
legend('1','2','3','4','5','6')
title('Trajectories','FontWeight','bold','FontSize',15)
xlabel('x [\mum]','FontSize',10)
ylabel('y [\mum]','FontSize',10)
% xlim([a*1e+6 b*1e+6])
% ylim([a*1e+6 b*1e+6])


%
% Plot of individual particle trajectories
figure;

% 1st particle
subplot(3,2,1)
hold on
plot(px(1,:)*1e+6,py(1,:)*1e+6)
plot(px(1,1)*1e+6,py(1,1)*1e+6,'o','MarkerSize',30,'Color','r')
plot(px(1,N)*1e+6,py(1,N)*1e+6,'*','MarkerSize',30,'Color','r')
hold off
```

```
title('1^{st} particle','FontWeight','bold','FontSize',15)
xlabel('x [\mum]','FontSize',10)
ylabel('y [\mum]','FontSize',10)
% xlim([a*1e+6 b*1e+6])
% ylim([a*1e+6 b*1e+6])

% 2nd particle
subplot(3,2,2)
hold on
plot(px(2,:)*1e+6,py(2,:)*1e+6)
plot(px(2,1)*1e+6,py(2,1)*1e+6,'o','MarkerSize',30,'Color','r')
plot(px(2,N)*1e+6,py(2,N)*1e+6,'*','MarkerSize',30,'Color','r')
hold off
title('2^{nd} particle','FontWeight','bold','FontSize',15)
xlabel('x [\mum]','FontSize',10)
ylabel('y [\mum]','FontSize',10)
% xlim([a*1e+6 b*1e+6])
% ylim([a*1e+6 b*1e+6])

% 3rd particle
subplot(3,2,3)
hold on
plot(px(3,:)*1e+6,py(3,:)*1e+6)
plot(px(3,1)*1e+6,py(3,1)*1e+6,'o','MarkerSize',30,'Color','r')
plot(px(3,N)*1e+6,py(3,N)*1e+6,'*','MarkerSize',30,'Color','r')
hold off
title('3^{rd} particle','FontWeight','bold','FontSize',15)
xlabel('x [\mum]','FontSize',10)
ylabel('y [\mum]','FontSize',10)
% xlim([a*1e+6 b*1e+6])
% ylim([a*1e+6 b*1e+6])

% 4th particle
subplot(3,2,4)
hold on
plot(px(4,:)*1e+6,py(4,:)*1e+6)
plot(px(4,1)*1e+6,py(4,1)*1e+6,'o','MarkerSize',30,'Color','r')
plot(px(4,N)*1e+6,py(4,N)*1e+6,'*','MarkerSize',30,'Color','r')
hold off
title('4^{th} particle','FontWeight','bold','FontSize',15)
```

```
xlabel('x [\mum]','FontSize',10)
ylabel('y [\mum]','FontSize',10)
% xlim([a*1e+6 b*1e+6])
% ylim([a*1e+6 b*1e+6])

% 5th particle
subplot(3,2,5)
hold on
plot(px(5,:)*1e+6,py(5,:)*1e+6)
plot(px(5,1)*1e+6,py(5,1)*1e+6,'o','MarkerSize',30,'Color','r')
plot(px(5,N)*1e+6,py(5,N)*1e+6,'*','MarkerSize',30,'Color','r')
hold off
title('5^{th} particle','FontWeight','bold','FontSize',15)
xlabel('x [\mum]','FontSize',10)
ylabel('y [\mum]','FontSize',10)
% xlim([a*1e+6 b*1e+6])
% ylim([a*1e+6 b*1e+6])

% 6th particle
subplot(3,2,6)
hold on
plot(px(6,:)*1e+6,py(6,:)*1e+6)
plot(px(6,1)*1e+6,py(6,1)*1e+6,'o','MarkerSize',30,'Color','r')
plot(px(6,N)*1e+6,py(6,N)*1e+6,'*','MarkerSize',30,'Color','r')
hold off
title('6^{th} particle','FontWeight','bold','FontSize',15)
xlabel('x [\mum]','FontSize',10)
ylabel('y [\mum]','FontSize',10)
% xlim([a*1e+6 b*1e+6])
% ylim([a*1e+6 b*1e+6])
%

%
% Mean square displacement of particle trajectories
figure;
plot(u,msd*1e+12);
xlabel('Lag Time [s]','FontSize',10)
ylabel('MSD [\mum^2]','FontSize',10)
title('Mean Squared Displacement','FontWeight','bold','FontSize',15)
```

```
figure;

subplot(5,2,[1 2 3 4])
hold on;
plot(u,msd(1,:)*1e+12);
plot(u,msd(2,:)*1e+12,'k');
plot(u,msd(3,:)*1e+12,'r');
plot(u,msd(4,:)*1e+12,'g');
plot(u,msd(5,:)*1e+12,'y');
plot(u,msd(6,:)*1e+12,'m');
hold off;
legend('1','2','3','4','5','6');
xlabel('Lag Time [s]','FontSize',10)
ylabel('MSD [\mum^2]','FontSize',10)
title('Mean Squared Displacement','FontWeight','bold','FontSize',15)

subplot(5,2,5)
loglog(u,msd(1,:)*1e+12);
xlabel('Lag Time [s]','FontSize',10)
ylabel('MSD [\mum^2]','FontSize',10)
title('MSD of 1^{st} particle','FontWeight','bold','FontSize',10)

subplot(5,2,6)
loglog(u,msd(2,:)*1e+12,'k');
xlabel('Lag Time [s]','FontSize',10)
ylabel('MSD [\mum^2]','FontSize',10)
title('MSD of 2^{nd} particle','FontWeight','bold','FontSize',10)

subplot(5,2,7)
loglog(u,msd(3,:)*1e+12,'r');
xlabel('Lag Time [s]','FontSize',10)
ylabel('MSD [\mum^2]','FontSize',10)
title('MSD of 3^{rd} particle','FontWeight','bold','FontSize',10)

subplot(5,2,8)
loglog(u,msd(4,:)*1e+12,'g');
xlabel('Lag Time [s]','FontSize',10)
ylabel('MSD [\mum^2]','FontSize',10)
title('MSD of 4^{th} particle','FontWeight','bold','FontSize',10)
```

```
subplot(5,2,9)
loglog(u,msd(5,:)*1e+12,'y');
xlabel('Lag Time [s]','FontSize',10)
ylabel('MSD [\mum^2]','FontSize',10)
title('MSD of 5^{th} particle','FontWeight','bold','FontSize',10)

subplot(5,2,10)
loglog(u,msd(6,:)*1e+12,'m');
xlabel('Lag Time [s]','FontSize',10)
ylabel('MSD [\mum^2]','FontSize',10)
title('MSD of 6^{th} particle','FontWeight','bold','FontSize',10)
%



%
% Cross correlation functions
figure;

subplot(3,2,1)
[c,lags] = xcorr(px(1,:)*1e+6,px(2,:)*1e+6);
plot(lags,c);
xlabel('Lag time [s]','FontSize',10);
ylabel('Cross correlation','FontSize',10);
title('Correlation of 1^{st} and 2^{nd} particle in x',...
    'FontWeight','bold','FontSize',13);

subplot(3,2,2)
[c,lags] = xcorr(px(1,:)*1e+6,px(3,:)*1e+6);
plot(lags,c);
xlabel('Lag time [s]','FontSize',10);
ylabel('Cross correlation','FontSize',10);
title('Correlation of 1^{st} and 3^{rd} particle in x',...
    'FontWeight','bold','FontSize',13);

subplot(3,2,3)
[c,lags] = xcorr(px(2,:)*1e+6,px(3,:)*1e+6);
plot(lags,c);
xlabel('Lag time [s]','FontSize',10);
ylabel('Cross correlation','FontSize',10);
title('Correlation of 2^{nd} and 3^{rd} particle in x',...
```

```
    'FontWeight','bold','FontSize',13);

subplot(3,2,4)
[c,lags] = xcorr(px(2,:)*1e+6,px(6,:)*1e+6);
plot(lags,c);
xlabel('Lag time [s]','FontSize',10);
ylabel('Cross correlation','FontSize',10);
title('Correlation of 2^{nd} and 6^{th} particle in x',...
    'FontWeight','bold','FontSize',13);

subplot(3,2,5)
[c,lags] = xcorr(px(4,:)*1e+6,px(5,:)*1e+6);
plot(lags,c);
xlabel('Lag time [s]','FontSize',10);
ylabel('Cross correlation','FontSize',10);
title('Correlation of 4^{th} and 5^{th} particle in x',...
    'FontWeight','bold','FontSize',13);

subplot(3,2,6)
[c,lags] = xcorr(py(4,:)*1e+6,py(5,:)*1e+6);
plot(lags,c);
xlabel('Lag time [s]','FontSize',10);
ylabel('Cross correlation','FontSize',10);
title('Correlation of 4^{th} and 5^{th} particle in y',...
    'FontWeight','bold','FontSize',13);
%


%% Coda

toc
```